Norwegian
Meteorological
Institute

Evaluation of the FjordOs-model

FjordOs technical report No. 4

Karina Hjelmervik[1]**, Nils M. Kristensen**[2]
Lars P. Røed[2,3]**, André Staalstrøm**[4]

Norwegian
Meteorological
Institute

HSN Høgskolen
i Sørøst-Norge

NIVA
Norsk institutt for vannforskning
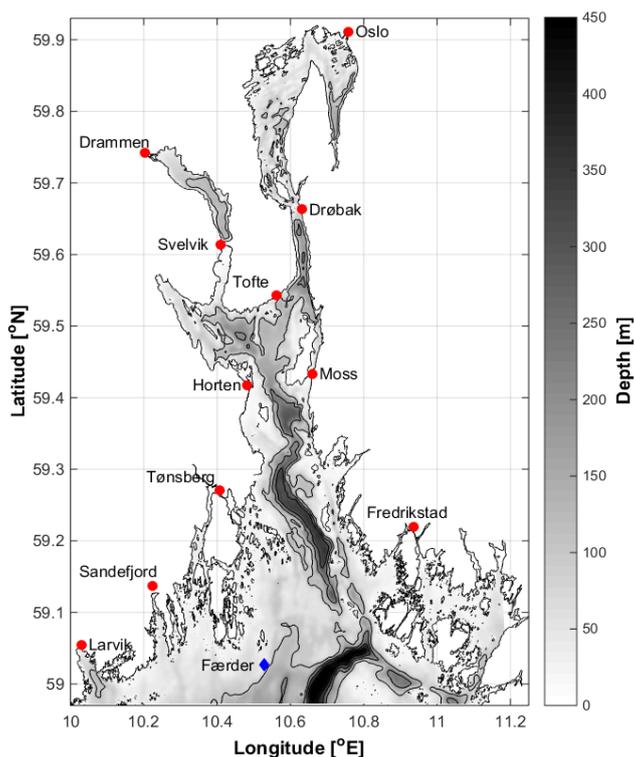
[1]University College of Southeast Norway, [2]Norwegian Meteorological Institute,

[3]Department of Geosciences, University of Oslo, [4]Norwegian Institute for Water Research

Norwegian Meteorological Institute

METreport

Title	Date
Evaluation of the FjordOs-model: FjordOs technical report No. 4	June 15, 2017
Section	**Report no.**
Ocean and Ice	11/2017
Author(s)	**Classification**
Karina Hjelmervik, Nils Melsom Kristensen, Lars Petter Røed, André Staalstrøm	● Free ○ Restricted
Client(s)	**Client's reference**

Abstract

Provided is an evaluation on the performance of the FjordOs model, a new circulation model covering the Oslofjord, Norway. The model is developed to improve the ocean input (e.g., currents) to emergency models used to predict pathways of oil and/or other effluents. The FjordOs model is a regional adaption of the Regional Ocean Modeling System (ROMS), and makes use of the model's curvilinear option to increase the resolution without inflating the computer demand significantly. To assess the model's rendition of the circulation we compare results from a simulation near two years long to available observations. The observations encompass water level, currents and temperature at various time periods at fixed stations, and observed trajectories of drifters. The evaluation reveals that the model is not perfect, but nevertheless we argue that its performance is adequate for its purpose. An important justification is that the higher resolution offers a decrease in the number of stranded trajectories compared to models of coarser resolution. Also of importance is that the model provides a realistic depth profile of the currents, and the tidal elevation.

Keywords

Ocean model, Oslofjord, ROMS, Validation, FjordOs

Disciplinary signature	Responsible signature
Bruce Hackett	Bruce Hackett

Abstract

Abstract

Provided is an evaluation on the performance of the FjordOs model, a new circulation model covering the Oslofjord, Norway. The model is developed to improve the ocean input (e.g., currents) to emergency models used to predict pathways of oil and/or other effluents. The FjordOs model is a regional adaption of the Regional Ocean Modeling System (ROMS), and makes use of the model's curvilinear option to increase the resolution without inflating the computer demand significantly. To assess the model's rendition of the circulation we compare results from a simulation near two years long to available observations. The observations encompass water level, currents and temperature at various time periods at fixed stations, and observed trajectories of drifters. The evaluation reveals that the model is not perfect, but nevertheless we argue that its performance is adequate for its purpose. An important justification is that the higher resolution offers a decrease in the number of stranded trajectories compared to models of coarser resolution. Also of importance is that the model provides a realistic depth profile of the currents, and the tidal elevation.

Contents

List of Figures

xi

xii

List of Tables

1   Introduction

We assess the performance of a new regional circulation model for the Oslofjord, Norway. The model is named FjordOs, and was recently developed specifically for the Oslofjord as detailed in *Røed et al.* (2016). The model is a version of the Regional Ocean Model System (ROMS) adapted for the fjord utilizing its curvilinear option.

The rationale behind the development of the the FjordOs model was to construct a model with high enough resolution to properly resolve the Oslofjord's highly irregular coastline and topography, and thereby resolve the fjord's many small islands, narrow straits and sounds as shown by Figure 1. The intended use of the model is to provide currents as input to a drift model to be able to forecast any drift of oil or other effluents to the fjord. Hence the model resolution must be high enough to avoid effluents stranding artificially when simulating their pathways from the source. As is well known currents, besides wind and waves, is one of the dominant sources when predicting pathways of effluents like oil and/or discharges of other contaminants. Thus, the FjordOs model is designed to deliver simulation and/or forecasts of water level, current, temperature and salinity accurate enough to be a useful input to drift models.

The evaluation is based on available observations for the two-year period 2014 and 2015 for which simulations with the FjordOs model is performed. Most of the observations are gathered from different sources independent of the FjordOs project, but also include measurements gathered during two short scientific cruises conducted by use of the research vessel (R/V) Trygve Braarud. The observations consist of measurements of water level, currents, temperature and salinity (CTD and water temperature at fixed stations), and trajectories of drifters (*Hjelmervik et al.*, 2016). Most of the data are scattered in time and space. Finally, some observations were performed close to Svelvik in 2015 in the Drammensfjord, a western branch of the main Oslofjord (*Staalstrøm and Hjelmervik*, 2017).

Section 2 gives a brief introduction to the Oslofjord and the model, while Section 3 offers details on the observations. The assessment of the model's performance is presented in Section 4, while a summary including conclusions and some final remarks are proffered in Section 5. Some calculations on drifting lanes from the Slagen refinery are added in the Appendix.

2   The Oslofjord and the FjordOs model

2.1   The Oslofjord

The area of interest, and the domain covered by the model FjordOs, is the Oslofjord including the Drammensfjord and the Inner Oslofjord (Fig. 1). The fjord is located in southeastern Norway

and is well described in the literature (e.g., *Baalsrud and Magnusson*, 2002; *Røed et al.*, 2016; *Hjelmervik et al.*, 2017). Here we merely point out some salient facts that should be kept in mind when establishing a circulation model aimed at providing pathways of various effluents to the fjord.

As revealed by Figure 1, the fjord is rather long and narrow with occasional wider parts. At about 59.5°N the fjord splits in two branches. A western branch tapers into a narrow strait at Svelvik before it opens up somewhat to form the Drammensfjord. An eastern branch forms the long and narrow Drøbak Sound, before it also opens up to form the Inner Oslofjord with its characteristic "swan head". In the north south direction it is about 100 km long. At the entrance it is about 50 km wide, in the Drøbak Sound about 1-2 km wide, and as narrow as 180 meters at Svelvik.
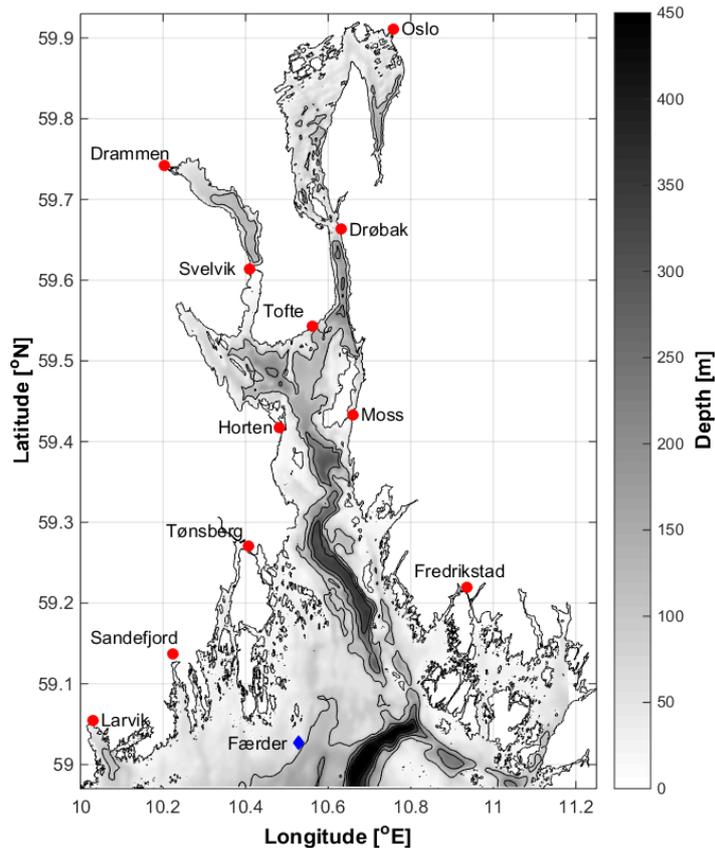
Figure 1: Displayed is the area covered by the Oslofjord and the FjordOs model. The red dots show the locations of some major and minor cities and villages along the coast, and which are mentioned in the text. The blue diamond indicates the position of the Færder Lighthouse close to the model's southern boundary.

Both branches have a sill. The sill in the eastern branch, the Drøbak Sill, is located close to the island Kaholmen which holds the citadel Oscarsborg. It consists partly of a man made underwater jetty only 1-2 meters deep extending halfway across the fjord from the western side. East of the jetty there is a natural sill of about 20 meters depth. Due its narrowness and shallowness the Drøbak Sill area is famous for its strong tidal currents, which easily exceeds 1 m/s even though the mean total tidal amplitude is less than 20 cm. The sill in the western branch is rather long and narrow, about 1 km long and 180 meters wide. The minimum depth is as shallow as 11 meters. This sill also causes a strong tidal current called the Svelvikstraum. North of the sills the maximum depth is more than 120 meters in both branches.

In addition to the existence of many small and large islands giving rise to many narrow sounds and straits, the fjord also have several deep basins ranging from 190 to 400 meters depths. Moreover, the fjord also exhibit a rather irregular coastline, and several rivers discharging fresh water into the fjord. Among the latter are two of Norway's largest rivers, namely Glomma (near Fredrikstad) and Drammenselva (near Drammen). An important contributer to the water level variations and thereby the circulation pattern in the fjord is the impact of events in the Skagerrak/North Sea through the Oslofjord's southern perimeter. For instance are storm surge events with amplitudes of one meter and higher observed in the fjord, which are associated with wind and pressure events in the Skagerrak/North

2.2 The FjordOs model

These complexities all contributes to a compounded circulation pattern, a pattern that is important to resolve when designing a circulation model for the fjord aimed at providing as realistic as possible pathways of effluents. To conceivably account for all these complexities and at the same time not exceeding the available computer capacities we opted to adapt the Rutgers Regional Ocean Modeling System (ROMS) when constructing the model for the Oslofjord, and to exploit its curvilinear option. ROMS is a publicly available ocean model featuring a terrain-following vertical coordinate and a free-surface. It is well documented by *Haidvogel et al.* (2008) and by *Shchepetkin and McWilliams* (2003, 2005, 2009). The particular version adapted to the Oslofjord is called FjordOs. For details on the FjordOs model and the simulations performed for the two years 2014 and 2015 the reader is referred to *Røed et al.* (2016). The latter also describes the setup including the applied external inputs, such as atmospheric input, river input, tidal input, and the input of sea level, currents and hydrography at the model's open lateral southern boundary.

Finally we emphasize that since ROMS is a terrain-following model it is plagued by currents created by the inescapable pressure gradient error (*Haney*, 1991; *Berntsen and Thiem*, 2007). To minimize its effect we have, as is common, smoothed the topography to avoid excessive pressure gradient errors to appear. Thus the real Oslofjord topography differs from the model topography.

The effect is to lessen the gradient of steep slopes, for instance close to the coastline and at shelf breaks of the deeper basins. This should be kept in mind when comparing model results and observations.

3 Observations

Model simulations are performed for the period April 2014 through December 2015. Locations of observations available for this period, are shown by Figure 2. They encompass water level as detailed in Section 3.1, profiles of currents (Section 3.2), temperature and salinity (Section 3.3), and temperature at fixed positions (Section 3.4). Also data from the Godafoss oil spill in February 2011 are available to us (Section 3.5). These observations are all gathered independent of the FjordOs project, and most of them are scattered in time and space. The exceptions are water level at Viker, Oscarsborg and Oslo and currents at Slagen. They are gathered regularly in time and for a much longer period. Finally, through the FjordOs project, we have collected surface drifter trajectory data during two cruises, one in September 2014 and another in September 2015 as detailed in Section 3.6.
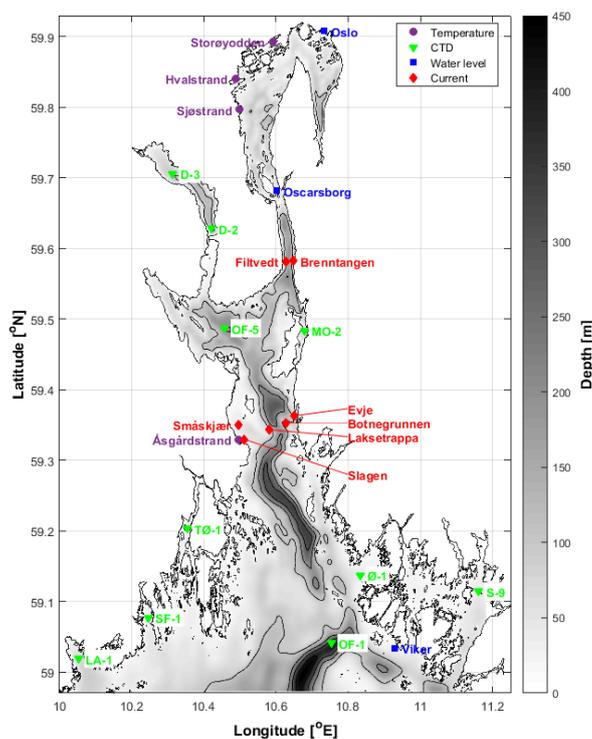
Figure 2: Names and locations where observations independent of the FjordOs project are available for the simulation period. Dark purple solid circles correspond to fixed temperature stations, green triangles to hydrographic stations (CTD stations), blue squares to water level stations, and red diamonds to moorings equipped with an Acoustic Doppler Current Profiler (ADCP).

3.1 Water level

The Norwegian Mapping Authority has three permanent stations measuring sea level in the Oslofjord (Figure 2), namely Viker, Oscarsborg and Oslo. As shown the station at Viker is located close to the open boundary of the model area, while Oscarsborg is located halfway into the Inner Oslofjord. The station Oslo is located in the Oslo Harbour. The station Viker was used to adjust the tidal input to the FjordOs model in accord with *Hjelmervik et al.* (2017).

3.2 Currents

3.2.1 Statnett moorings

During the period mid September through late November 2014 six moorings, each fitted with an upward looking Acoustic Doppler Current Progiler (ADCP), were deployed in the positions shown by Figure 2. Information about mooring reference, names and locations of these moorings (in terms of latitude and longitude) and instrument type are tabulated by Table 1. Two of the moorings (Filtvedt and Brenntangen) were deployed at the entrance to the Drøbak Sound. The remaining four (Småskjær, Laksetrappa, Botnegrunnen, and Evje) were deployed further south forming an east-west section across the fjord along a line with deep basins on either side (Figure 2). The moorings were all deployed as part of a project conducted by Statnett, NIVA, Akvaplan NIVA, and the University of Oslo (UiO). The R/V Trygve Braarud, UiO was used during deployment and recovery of the moorings. For further details about the moorings and corresponding instruments the reader is referred to *Staalstrøm and Ghaffari* (2015).

3.2.2 ExxonMobil mooring

Data from an additional bottom-mounted ADCP, named Slagen (Figure 2), and made available to us by ExxonMobil, Slagentangen, is also used for comparison with model results. It has measured currents regularly at two depths since 1997, and is located northwest of Turning Dolphin at the Slagen Refinery as shown by Figure 3. Note the Bliksekilen nature reserve, which is a shallow water area with rare flora and fauna, which is located west of the Slagen Refinery.

3.3 CTD measurements

On behalf of Fagrådet for Ytre Olsofjord NIVA collects CTD measurements at a number of selected positions in the Oslofjord. The work is part of a program monitoring the eutrophication state of the Outer Oslofjord and the Drammensfjord. The data collected are available through a web portal[1]. We use data from ten of these as listed by Table 2. Their resepctive locations are

---

[1]http://www.aquamonitor.no/ytreoslofjord/

Table 1: Target positions (WGS84) of the Statnett ADCP current instrument moorings. Depths at the stations are from the Statnett terrain model. Note that the model depth at the same location may differ due to the smoothing of the model topography.

Mooring ref	Name	Latitude [^{o}N]	Longitude [^{o}E]	Depth [m]	Instruments
Kp11.2 (Ri1)	Småskjær	59.350124	10.497661	20	Aquadopp600 AQP1531 Transducer LRT2
Kp5.7 (Rl1)	Laksetrappa	59.343452	10.581023	75	Aquadopp400 AQP4689 Transducer LRT3 Aanderaa Seaguard
Kp2.6 (Rm1)	Botnegrunnen	59.352375	10.626822	96	Continental WAV6117 Transducer LRT4
Kp0.7 (Rn1)	Evje	59.363182	10.653576	64	Aquadopp400 AQP2931 Transducer LRT5
Kn2	Brenntangen	59.581803	10.646087	54	Aquadopp400 AQP5608 Transducer LRT6
Km1	Filtvedt (current)	59.582064	10.627372	153	Continental CNL6037 Transducer 207-2
Km2	Filtvedt (temperature)	59.580778	10.626239	125	TinyTags UIO1-7 Transducer 203-2

shown in Fig. 2 as green triangles. The measurements include profiles of temperature and salinity as well as water quality parameters. During the simulation period April 2014 through December 2015 12 CTD profiles was available covering the months January, February, June, July, August, September, and November. No data are unfortunately available in spring and early summer.

We note that only a few of the CTD stations are located in the open part of the fjord. In fact seven of the ten stations are located inside narrow straits and sounds, or inside lesser subfjords or inlets. Of the remaining three stations only two are in the open parts of the fjord, namely Torbjørnskjær (OF-1) and Breiangen (OF-5), while the last (Ø-1) is positioned in a semi-open location west of the Hvaler Archipelago. The latter is interesting in that it is influenced by the fresh water discharged by the western branch of the river Glomma. In this respect also the stations D-2 and D-3 are interesting being located inside the sill in the Drammensfjord in which the river Drammenselva discharges its fresh water.

3.4 Temperature measurements
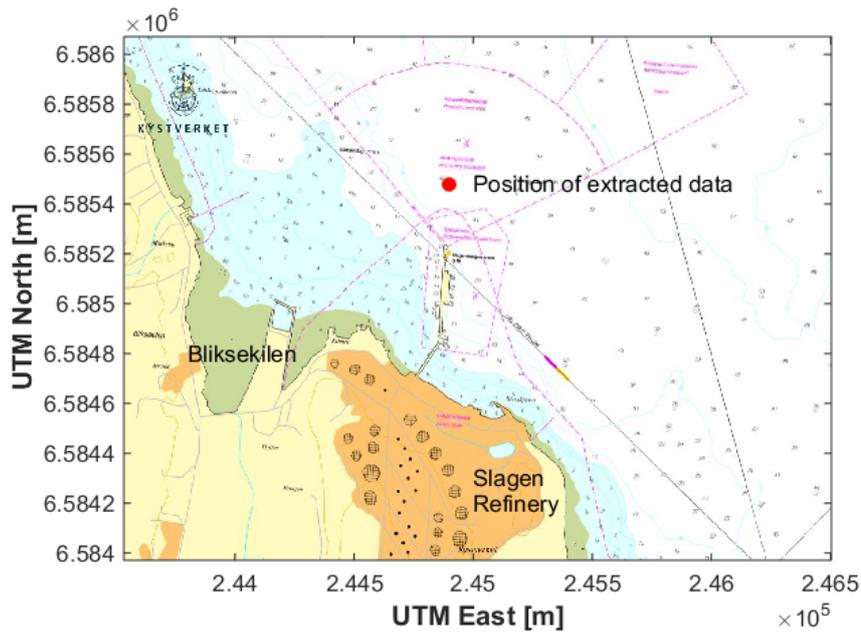
Figure 3: Zoom in of the location of the bottom-mounted ADCP close to the Slagen Refinery (red dot). Source: Norwegian Coastal Administration.

Temperature measurements at four fixed position are available to us. One of them is oerated by Scanmar AS and is located three kilometres south of Åsgårdstrand (Figure 2). The remaining three are located in the Inner Oslofjord (Figure 4).

3.4.1 The Scanmar mooring

The Scanmar mooring measures temperature hourly at one meter depth, and has done so over the last ten years. The device has an accuracy of $\pm 0.15^{\circ}$C in the range from -5 to +30°C.

3.4.2 Temperatures in the Inner Oslofjord

In addition to the Scanmar mooring we have access to temperature measurements at three beaches in the Inner Oslofjord, namely Sjøstrand, Hvalstrand and Storøyodden (Figure 4). These measurements are the result of a collaboration between Asker and Bærum kommune and Finnerud Elektronikk. The measurement device is a digital thermometer (Maxim Integrated DS18B20) with an accuracy of $\pm 0.5^{\circ}$C. They measure water temperature at 40 cm beneath the surface in water depths of several meters. Temperatures are measured every three hours from 09:00 to 18:00 during the summer months. We note that the site Sjøstrand is the only one located in a semi-open position, while the two other beaches are well within archipelagoes that are somewhat sheltered

Table 2: Positions (latitude, longitude) and number of profiles taken at each of the ten CTD measurement sites used.

Tag	Station	Latitude	Longitude	Number of measurements	
		[^{o}N]	[^{o}E]	2014	2015
D-2	Inner Drammensfjord	59.6280	10.4210	5	7
D-3	Solumstrand	59.7060	10.3140	5	6
LA-1	Larviksfjord	59.0190	10.0520	5	7
MO-2	Kippenes	59.4840	10.6780	5	7
OF-1	Torbjørnskjær	59.0410	10.7540	5	7
OF-5	Breiangen	59.4870	10.4580	5	7
S-9	Haslau, Singlefjord	59.1140	11.1620	7	10
SF-1	Sandefjord	59.0770	10.2460	5	7
TØ-1	Vestfjord	59.2030	10.3550	5	7
Ø-1	Leira. Vesterelva	59.1370	10.8340	7	10

from the rest of the fjord.

3.5 Godafoss oil spill

On Thursday the 17th of February 2011 at 19:52 local time, the containership Godafoss ran aground at the Kværnskjærgrunnen rock in Løperen. It us located between the islands of Asmaløy and Kirkøy in the Hvaler municipality in southeastern Norway (Figure 5). One of the effects of this grounding was an acute release of oil from the ship, which drifted westward from the accident site. The oil slick has been observed from aeroplane by the Norwegian Coastal Administration (Kystverket), and the sites where stranded oil has been observed, are also registered (Figure 5). This accident was on of the motivation factors for the project FjordOs, and hence, although no simulations are performed for this particular event, we will, nevertheless simulate trajectories from this location using the simulations performed for the period April 2015 through December 2015 (Section 4).

At the time of the grounding there were clear skies and temperatures around -3°C. Observations of wind from Strømtangen lighthouse (15 km away from the grounding site) indicate 6-7 m/s winds from the north-east.

3.6 Surface drifters
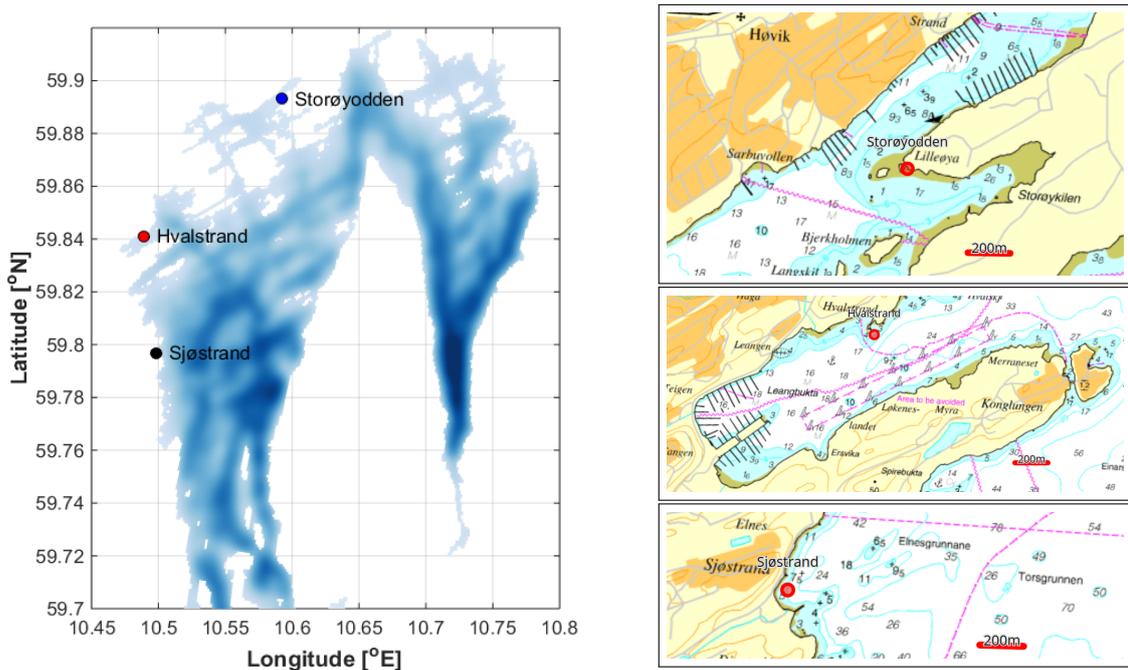
Figure 4: The positions at three beaches in the Inner Oslofjord where the temperature measurements are performed.

As part of the FjordOs project two cruises in the Oslofjord were performed. During these cruises a total number of 15 surface drifters were released (Figure 6). Two were released during a cruise in September 2014, and the remaining 13 was released in a cruise in September 2015 (Figure 7). The second cruise is documented in *Hjelmervik et al.* (2016), which also describes the drifters used in detail. The focus area of the drifter campaigns is the Breiangen area, and the area between Horten and Moss.
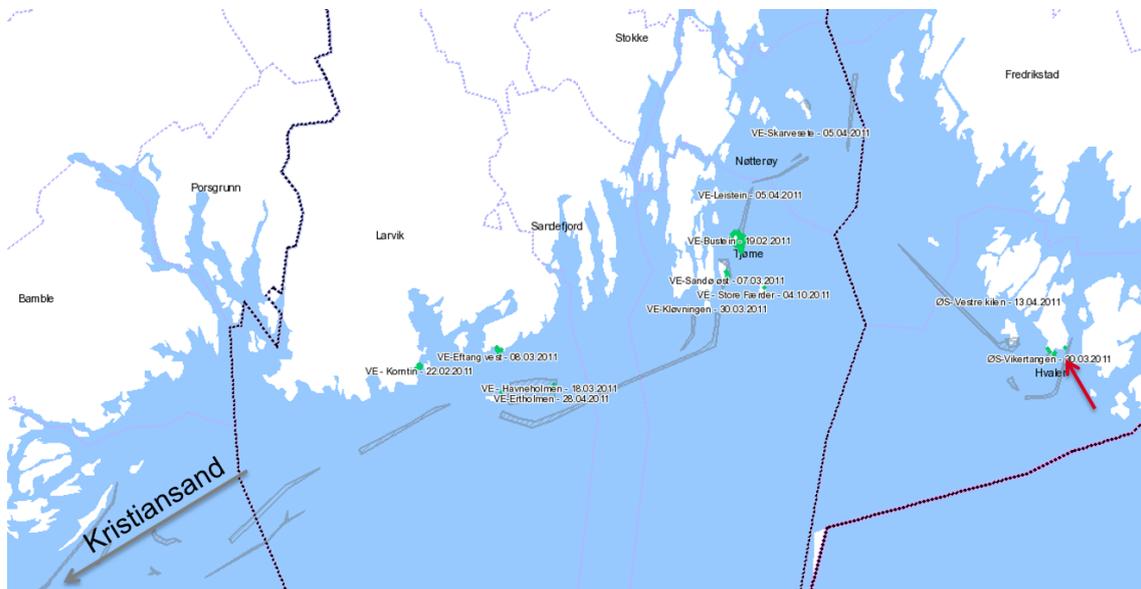
Figure 5: The observed oil spill from the Godafoss accident 17th of February 2011. The red arrow on the right-hand side indicates the grounding position (Kværnskjærgrunnen). The grey areas are oil slicks observed from aircraft, while green areas indicate stranded oil. The name of the locations where oil was observed and at which time are included as text. Source: The Norwegian Coastal Administration

Figure 6: The "home-made" drifters on the deck of the R/V Trygve Braarud (left-hand panel) and in the water after deployment (right-hand panel). In all 15 of these were dropped and tracked during the FjordOs project, two in 2014 and 13 in 2015.
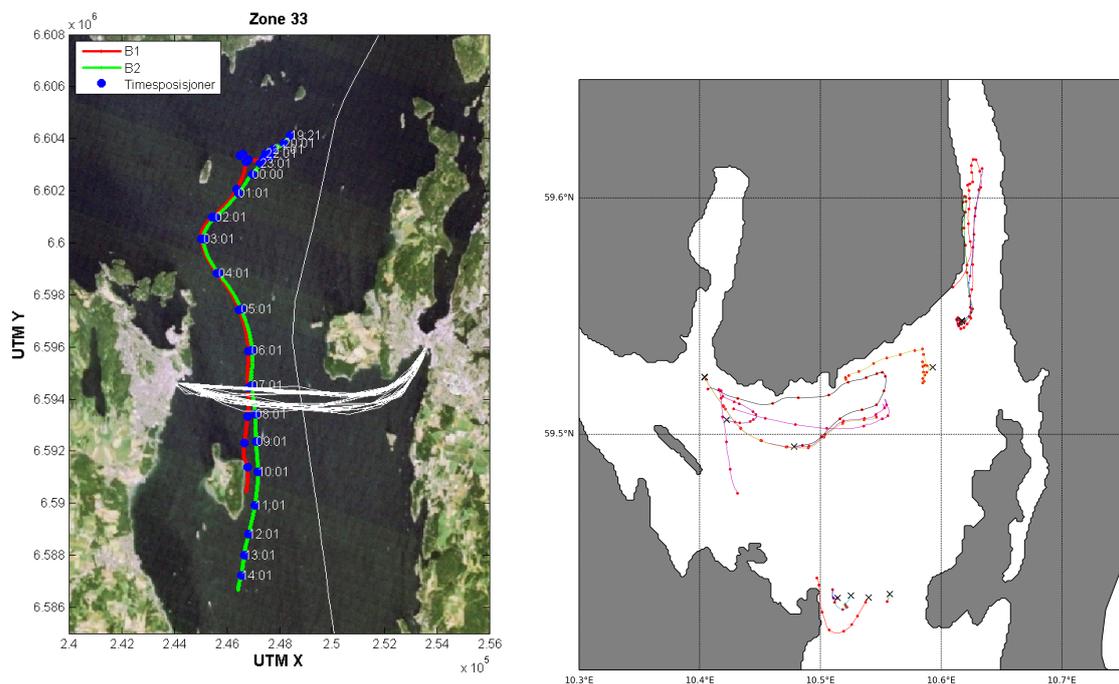
Figure 7: Trajectories of the two drifters released in September 2014 (left-hand panel) and the 13 drifters released in September 2015 (right-hand panel).

4 Evaluation

4.1 Water level and tide

Time series of water level from the three tide gauge stations (Section 3.1) were extracted for the period April 2014 through December 2015. To evaluate the model performance we also extracted time series of water level at locations near the three stations from the model simulation for the same time period. We emphasize that the tidal forcing we used at the southern open boundary of the FjordOs model includes eleven tidal constitutents only, and that the tidal forcing was adjusted by use of the observed tide at Viker close to the southern boundary (*Røed et al.*, 2016).

To compare model and observation we first analysed the two time series by use of t_tide (*Pawlowicz et al.*, 2002) to extract the amplitudes and phases of the individual harmonic tidal components. Next we superimposed the water elevation due to each of the eleven tidal constituents included in the tidal forcing to obtain what we term the combined water elevation. We finally subtracted the resulting combined water elevation from the total water elevation of each time series to derive comparabel "residual" water elevations.

As revealed by Figure 8 the combined water elevation compares favourably with the observation. This is also true for the residual, but to a lesser degree. The latter is to be expected since the observations include all the tidal water elevations due to tides of longer and shorter periods than the eleven included in the tidal forcing. Note that to be able to discriminate between observations and simulated water levels the time series shown by Figure 8 is truncated to January 2015.

Of the eleven tidal components included in the tidal forcing M2 is, in terms of amplitude, the dominant constituent. It is therefore noteworthy, as revealed by Table 3 on page 16, that the model represents this influential constituent to a very satisfactory degree both regarding amplitude and phase. This is true even at the stations Oscarsborg and Oslo that are both far from the models southern boundary. We also note that the constituents S2, N2 and O1 contribute, and that their contributions are in fairly good agreement with the observations as well.

Table 3 and Figure 9 also show that even the longer period tidal constituents, e.g., SS and SSA, are to some degree picked up by the model despite the fact that they are not incorporated in the tidal forcing. This may be explained by the fact that we in addition to the tides also use daily mean water level, hydrography and currents extracted from the NorKyst800 model as forcing on the southern boundary (*Røed et al.*, 2016). In contrast, and as expected tides of periods shorter than 6 hours are not picked up by the model at all (Figure 9).

Finally we note, as revealed by Table 3, that the observed M2 amplitude increases from south to north. This is reflected in the simulations as well as displayed by Figure 10. It is interesting to note that the lowest M2 amplitude is found in the Drammensfjord north of the threshold in
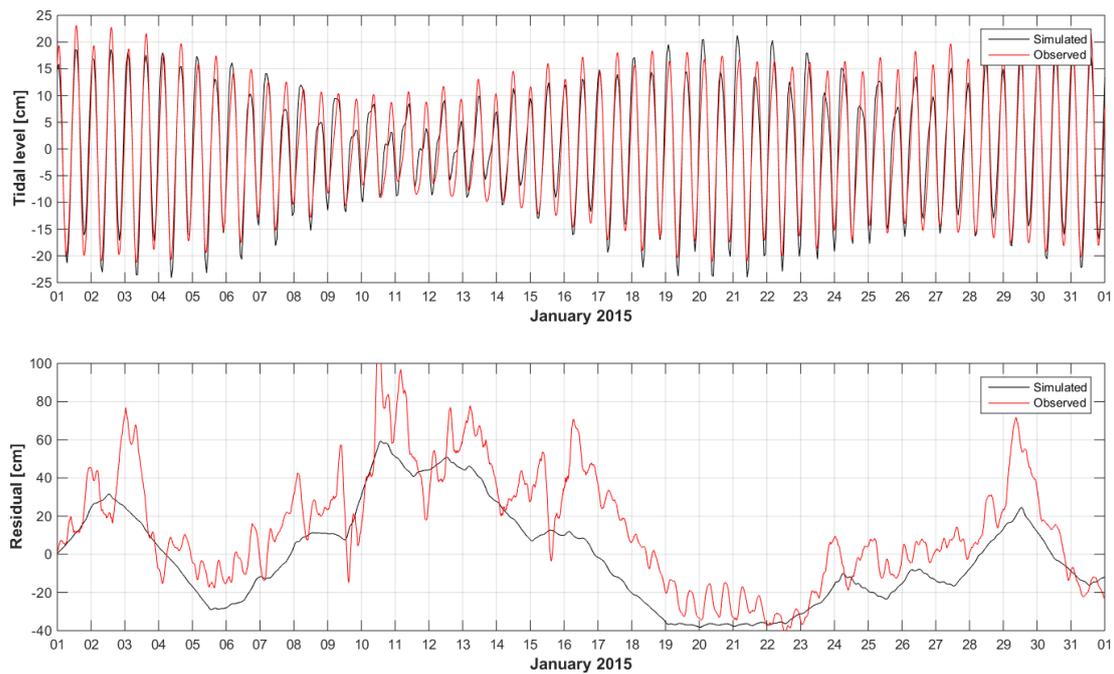
Figure 8: Simulated (black) and observed (red) time series of the combined tidal water elevation (upper panel) and residual water level (lower panel) at Oscarsborg (cf. Figure 2) for the month of January 2015.

Svelvik. In fact the M2 phase has a sudden increase at the thresholds of Svelvik and Drøbak. The same is true for the majority of the other relevant tidal components (not shown).
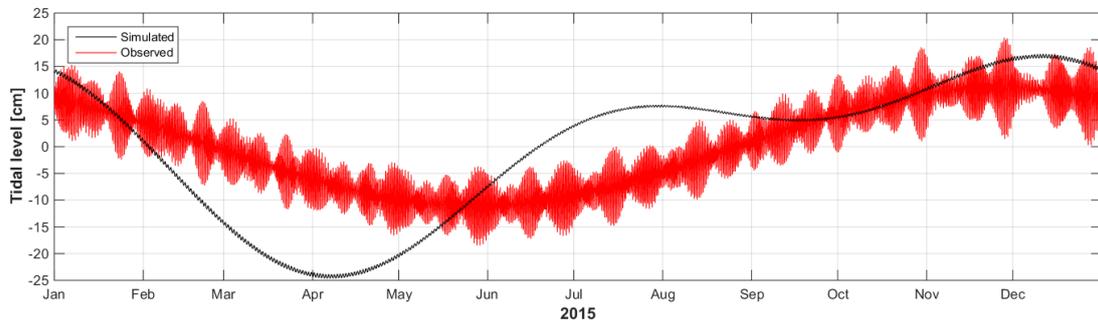
Figure 9: Time series at Oscarsborg of the tidal components not included in the tidal forcing.
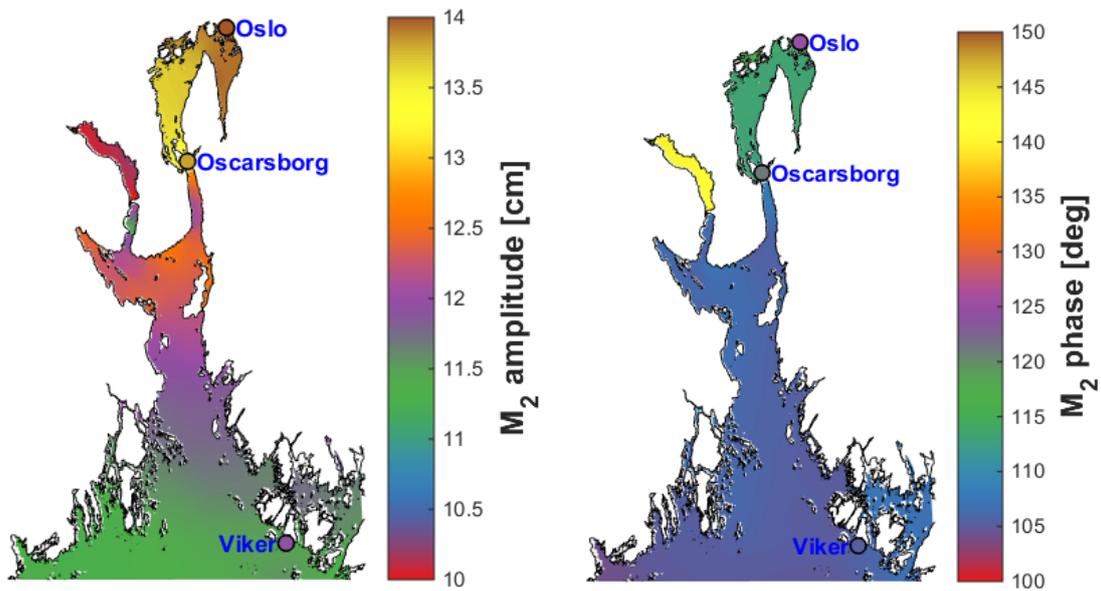
Figure 10: Simulated fields of M2 amplitude (left-hand panel) and phase (right-hand panel). Corresponding observed values for M2 amplitude and phase are marked with circles at Viker, Oscarsborg, and Oslo.

Table 3: Simulated and observed tidal amplitudes and phases at three tide gauge stations for selected tidal components sorted by period.

Comp.	Period [h]	sim/ obs	Viker amp. [cm]	Viker phase. [deg]	Oscarsborg amp. [cm]	Oscarsborg phase. [deg]	Oslo amp. [cm]	Oslo phase. [deg]	Included in tidal forcing
SA	8764	sim	15.5	284	15.6	286	15.4	286	no
		obs	10.0	319	11	322	11.4	324	
SSA	4382	sim	8.8	197	9.2	200	9.4	200	no
		obs	7.5	188	8.0	189	8.2	190	
Q_1	26.8684	sim	0.0	231	0.0	216	0.1	215	no
		obs	1.1	190	1.2	198	1.3	200	
O_1	25.8193	sim	3.5	337	3.8	339	3.8	339	yes
		obs	2.2	277	2.3	281	2.4	282	
P_1	24.0659	sim	0.6	322	0.6	334	0.7	342	yes
		obs	0.2	129	0.3	102	0.4	97	
K_1	23.9345	sim	0.2	187	0.1	175	0.2	157	yes
		obs	0.4	127	0.7	130	0.8	130	
N_2	12.6584	sim	3.0	69	3.5	75	3.7	76	yes
		obs	3.0	60	3.4	76	3.6	80	
M_2	12.4206	sim	11.5	105	13.2	112	13.9	114	yes
		obs	11.9	105	13.8	121	14.4	125	
S_2	12.0000	sim	3.3	64	3.9	69	4.2	70	yes
		obs	2.9	46	3.3	65	3.5	69	
K_2	11.9672	sim	1.6	10	2.0	13	2.1	15	yes
		obs	0.7	45	0.8	66	0.9	66	
MN_4	6.2692	sim	0.2	5	0.5	32	0.6	35	yes
		obs	0.4	249	0.6	289	0.7	297	
M_4	6.2103	sim	1.0	355	1.9	18	2.5	23	yes
		obs	1.2	281	1.8	324	2.3	332	
MS_4	6.1033	sim	0.6	80	1.2	107	1.6	111	yes
		obs	0.3	360	0.5	44	0.7	56	

4.2 Currents

4.2.1 Currents in the Oslofjord

In essence currents in the Oslofjord are caused by tides, wind, storm surges, and differences in density caused by differences in temperature and salinity. The tides are more often than not the most dominant current in the fjord. Moreover it moves the whole water column, transports large amounts of water in and out of the fjord, and fluctuates with same period as the tidal elevation. It is therefore stronger in narrower parts of the fjord like the Drøbak Sound, and in particular across the sills at Oscarsborg (the Drøbak Sill) and at Svelvik. Even though the mean total tidal amplitude is less than 20 cm in the Oslofjord, the tidal currents are up to 1 m/s due to the narrow straits and sill depths.

Wind forced currents are caused by the traction of the wind on the surface, and hence fluctuates with the meteorological conditions. It is strongest near the surface but decreases rapidly with depth through the surface friction layer (about 10 to 30 m depth depending on wind strength). The wind forced currents near the surface is about 1-2% of the wind speed, and usually has an angle of 20 degrees to the right of the wind.

The storm surge currents are due to water level variations caused by atmospheric wind and pressure forces. Like the wind forced currents it also fluctuates with the meteorological conditions. As with tides the storm surge currents affect the whole water column. An example is when an atmospheric low pressure passes over the area. The low air pressure cause water levels to rise and in addition the wind stress on the surface causes the water to a pile up of along the coast. If a storm surge event coincides with a high tide the water level may become unusually high and lead to uncommonly strong currents. In connection with storm surge events, amplitudes of 100 cm or higher are observed. One such extreme event happened in October 1987 when the water level in Oslo rose to 196 cm above normal water level.

Differences in density creates pressure differences which in turn forces the water to move. Density differences in the Oslofjord are created when rivers discharge freshwater into the fjord, when water masses of different density than the original fjord water enters from the open sea (Skagerrak), or dense water is upwelled locally for instance due to atmospheric winds. We may then measure currents at depth without this being observed at the surface. Vertical variations in depth may also be caused by bathymetry which may prevent the water mass from moving, even if a horizontal pressure gradient is present. For instance when Glomma and Drammenselva rivers discharge freshwater to the Oslofjord the resulting current entrains water with higher salinity from below, causing the volume flow to increase and the salinity to decrease. This is for example evident in (*Røed et al.*, 2016, Figure 20) where it is possible to trace the water from these two main rivers far out into the fjord. To conserve the volume, the entrainment of water leads to a counter current

17

below the surface layer transporting new water into the area, to compensate for the loss of volume that the seaward surface flow represents. The resulting flow pattern is one example of a baroclinic current, where the horizontal pressure varies with depth.

Another example of a density driven flow is the interaction between Skagerrak and the Oslofjord at the latter's open, southern boundary. The circulation in the Skagerrak is on average counter-clockwise with brackish outflow from the Baltic Sea (*Rodhe*, 1996; *Svendsen et al.*, 1996; *Albretsen and Røed*, 2010). This flow pattern generate horizontal pressure gradients near the mouth of the Oslofjord (*Baalsrud and Magnusson*, 1990), and by mechanisms described by *Klinck et al.* (1981) variation in the wind pattern generate mean density driven flow events that may be stronger than the tidal current, especially in the outer Oslofjord where the fjord is wide.

In summary the currents in the Oslofjord are complex and may be caused by a multitude of effects that may mutually cancel or enhance each other. As a result they are highly varying in time and in horizontal space as well as depth. To evaluate the model results we therefore find it useful to (i) split the currents into a depth independent part (henceforth referred to as the external or barotropic mode) and a depth dependent part (henceforth referred to as the internal or baroclinic mode), and (ii) separate the current into a slowly and a rapidly varying part as detailed for instance by *Røed and Fossum* (2004). Examples of barotropic current components are tidal currents and currents caused by storm surge events, while density driven currents are examples of baroclinic currents.

As is common we estimate the barotropic part by equaling it to the depth average current. The latter is defined by

$$\mathbf{u}_0 = \frac{1}{h} \int_{-h}^{0} \mathbf{u} dz, \tag{1}$$

where h is the total water depth and $\mathbf{u}$ is the total current at any depth z. The depth varying deviation, or baroclinic mode, at any depth, say $u_n(z)$, is then simply estimated by subtracting the depth average current from the total current, that is,

$$\mathbf{u}_n = \mathbf{u} - \mathbf{u}_0. \tag{2}$$

To estimate the slowly varying part of the currents we first note that the density driven baroclinic currents varies on a time scale much longer than the barotropic tidal and storm surge currents. To reveal or estimate the estuarine circulation or the mean baroclinic flow, say $\bar{\mathbf{u}}$, we may therefore simply make an average over a period much longer than the typical tidal period and wind periods, e.g., several days, that is,

$$\bar{\mathbf{u}} = \frac{1}{T} \int_{t-\frac{1}{2}T}^{t+\frac{1}{2}T} \mathbf{u} dt \tag{3}$$

where T is the averaging time period and t is time.

4.2.2 The Statnett moorings

As revealed by Figure 11 the fjord width at the first transect Filtvedt-Brenntangen (henceforth FB) is 1.8 km, while the second transect Småskjær-Evje (henceforth SE) is about 10 km wide. The deepest part of the FB transect is found in the middle with and observed depth of 208 m, while the deepest part of the SE transect is found to the east of the middle with an observed depth of 204 m.

Figure 11 also shows that the observed and modelled bathymetry do not coincide. In fact the observed slopes are everywhere steeper. This is caused by the necessity of smoothing the model bathymetry with respect to the real topography to avoid the so called pressure gradient error referred to in Section 2. As shown the result is that the model maximum/mimimum depths are shallower/deeper than the observed maximum/minimum depths. Note also that the positions where the model results are extracted (indicated by the white vertical lines) may differ somewhat from the true positions of the observations. For instance the tru position of the Station Km1 is a little to the west of the model Km1 position. In fact its true position is where the real bathymetry has the same depth as the model bathymetry.
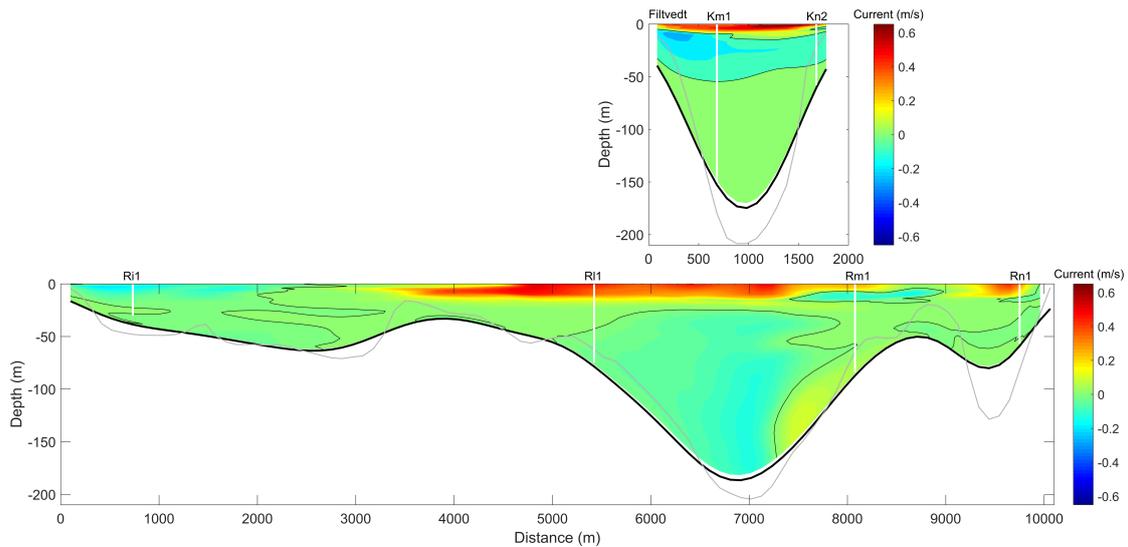
Figure 11: A snapshot of the simulated current speed across the two transect Filtvedt and Brenntangen (upper panel) and Småskjær-Evje (bottom panel). The location of the transects are shown in Figure 2. The bathymetry of the model is drawn with a thick black line, while the real bathymetry is drawn with a thin grey line. The simulated along fjord current speed in m/s, valid at October 24, 2014 at 12:00 UTC, is indicated by the colorbar. Here red colors indicate currents into the fjord, while blue colors indicate currents out of the fjord. A thin black line indicates where the current speed is zero. The white vertical lines indicate the position where model results are extracted for compariosn with the observations at the stations listed by Table 1.

The along fjord currents shown by Figure 11 are extracted when the mean flow is directed out of the fjord. At this instance the current through the FB transect is relativly uniform across the fjord, and observations at station Km1 can be said to be representaive for the whole transect. This is in contrast to the along fjord currents across the SE transect. Here it is evident that the current is not uniform across, and hence the observations at individual stations, for instance station Rl1, is not representative for the whole transect.

As alluded to the 3D current field is complex, and this is also captured by the FjordOs model. As an example Figure 12 shows the simulated currents at three different depths near Filtvedt. In general, the currents in the upper layer are stronger than further down. In the upper layers the currents are towards north, at 40 meters depth the currents towards south, and at 100 meters depth towards north again. Because of the complex flow pattern, the currents at a given coordinate is not necessarily representative for the whole area or transect. However, regarding the FB transect the currents across the fjord between station Km1 an Kn2 are relativly uniform except at 100 m depth. At 100 meters depth the currents at Filtvedt are weak and towards south even though the currents at 100 meters depth are generally stronger and towards north. At 40 meters depth the currents at Brenntangen is weaker than in the rest of the transect. Note that the depth at Brenntangen is 58 meters in the observations while the depth is only 46 meters at the corresponding point in the simulations due to the smoothing of the model bathymetry.
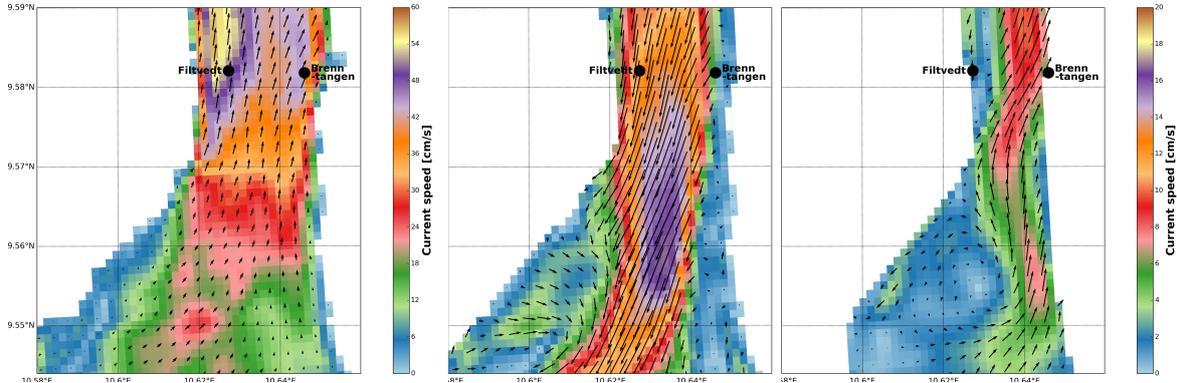
Figure 12: Simulated currents at 2 m (left), 40 m (middle), and 100 m (right) depth at 10th of October 2014 12:00. The colorbars gives the speed in m/s, while the arrows indicate the direction. Note that the middle and right panels shear colorbar. The figure emphasize the complex nature of the currents in the Oslofjord.

For a further detailed description of the observed current variability at the six stations forming the two transects we refer *Staalstrøm and Ghaffari* (2015). We note that they found that the tidal currents dominate in the FB transect, while the tidal currents across the SE transec are less pronounced and more or less masked by the mean flow. This due to the wideness of the the fjord

across the SE transect, which is five times wider there than width of the FB transect. This is also reflected in the simulated current, for instance by comparing the observed and simulated currents at the two stations Km1 (Figure 13), associated with the FB transect, and Rl1 (Figure 14), associated with the SE transect.
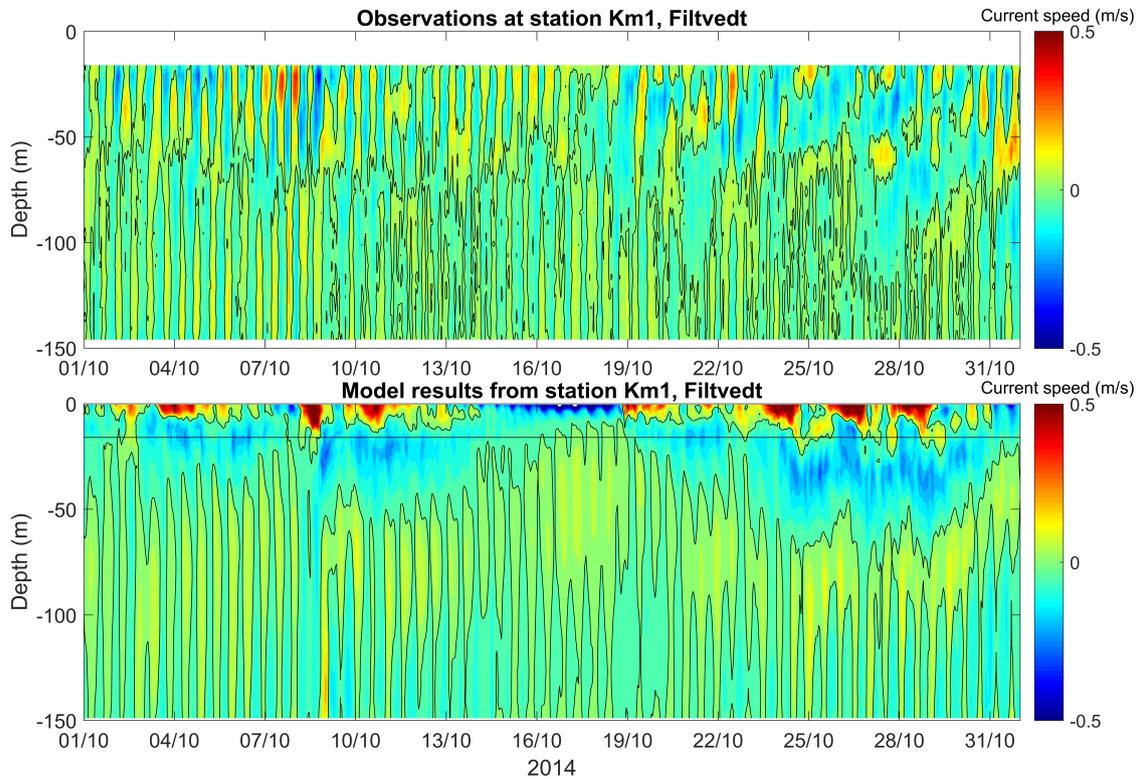
Figure 13: Observations (upper panel) and model results (lower panel) from station Km1 (FB transect). The colorbar indicates the current speed in m/s along the channel. Red colors indicate flow into the fjord, while blue colors indicate flow out of the fjord. The black contourline shows where the current speed is zero. Note that the shallowest observations is at 16 m depth, which is indicated by a straight horisontal line in the lower panel.

We have also estimated the mean flows of both the observed and the simulated currents at the two stations. In this we utilise (3) applying a running mean with a period of 49 hours. The result is shown by Figure 15 (FB transect) and Figure 16 (SE transect). We note that at the FB transect the model do not capture the mean flow correctly in that the mean flow is stronger in the model than in the observations. The model do however capture many of the baroclinic mean flow events observed at station Rl1 in the SE transect, in particular in the last part. It is promising that the model to some extent capture the mean flow events in the part of the fjord where this phenomena dominates. But it must be remarked that the model performance needs to be improved. These kind of events depends on the stratification in the model as well as fresh water input and the influence
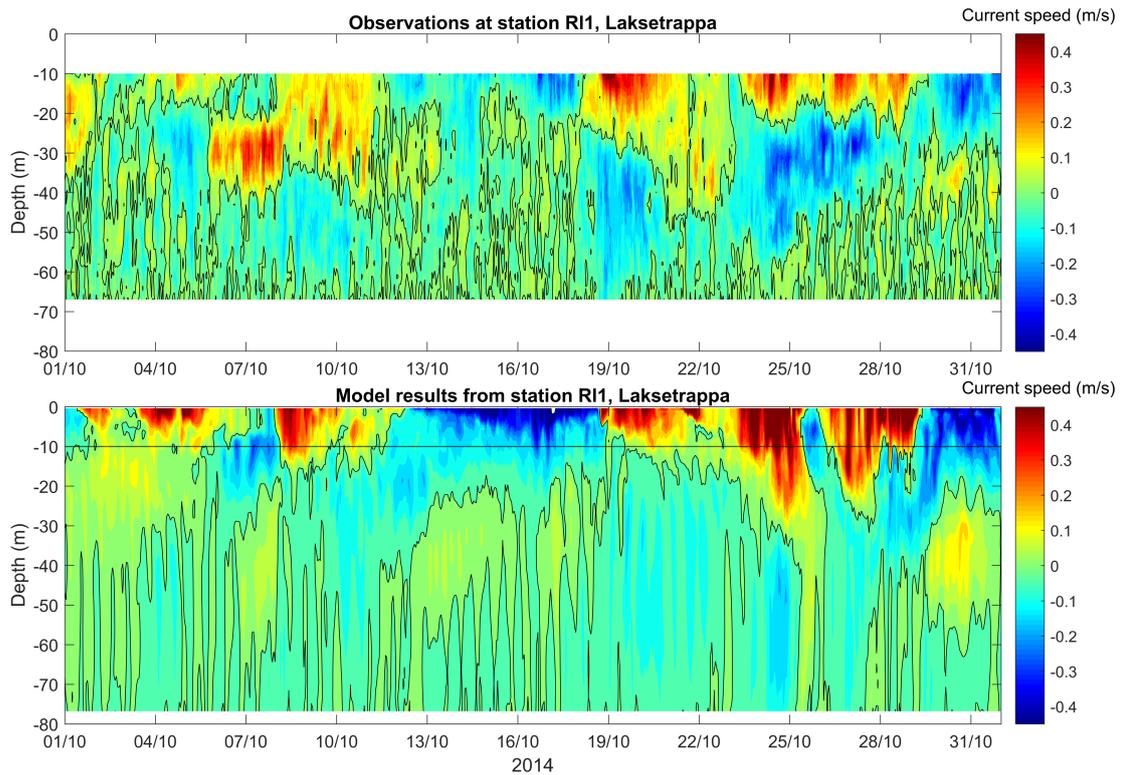
Figure 14: As Figure 13, but for Station Rl1 (SE transect). Here the shallowest observations is at 10 m depth.

from the open boundary. It is expected that model performance concerning mean flow will be improved if the stratification in the model is improved.

We now focus on the tidal currents in the FB transect at Station Km1 (Figure 17). To construct the figure we first subtract the mean flow ($\overline{\mathbf{u}}$), as shown in Figure 15, from the total flow leaving the residual parts (here denoted $\mathbf{u}'$). The tidal part ($\widetilde{\mathbf{u}}$) is then extracted from the $\mathbf{u}'$ time series exactly as described in Section 4.1 both for the observed and modelled currents by use of t_tide (*Pawlowicz et al.*, 2002) giving the tidal components for each depth. The time series is rather short and spans the period mid-September to the end of November 2014.

As displayed by Figure 17 the observation at station Km1 has a phase shift in the vertical structure of the current speed approximatly at about 55 m depth. This is the same depth at which a phase shift in the currents was reported by *Staalstrøm et al.* (2012) at a station close to Station Kn2 in September 2009. He found that the current in this location is influenced by internal tides generated at the Drøbak Sill propagating southward. The phase shift of the simulated current at Km1 is found somewhat deeper in the water column, in the depth range 80-100 m. This is an additional indication that the stratification in the model do not capture the real stratification correctly.
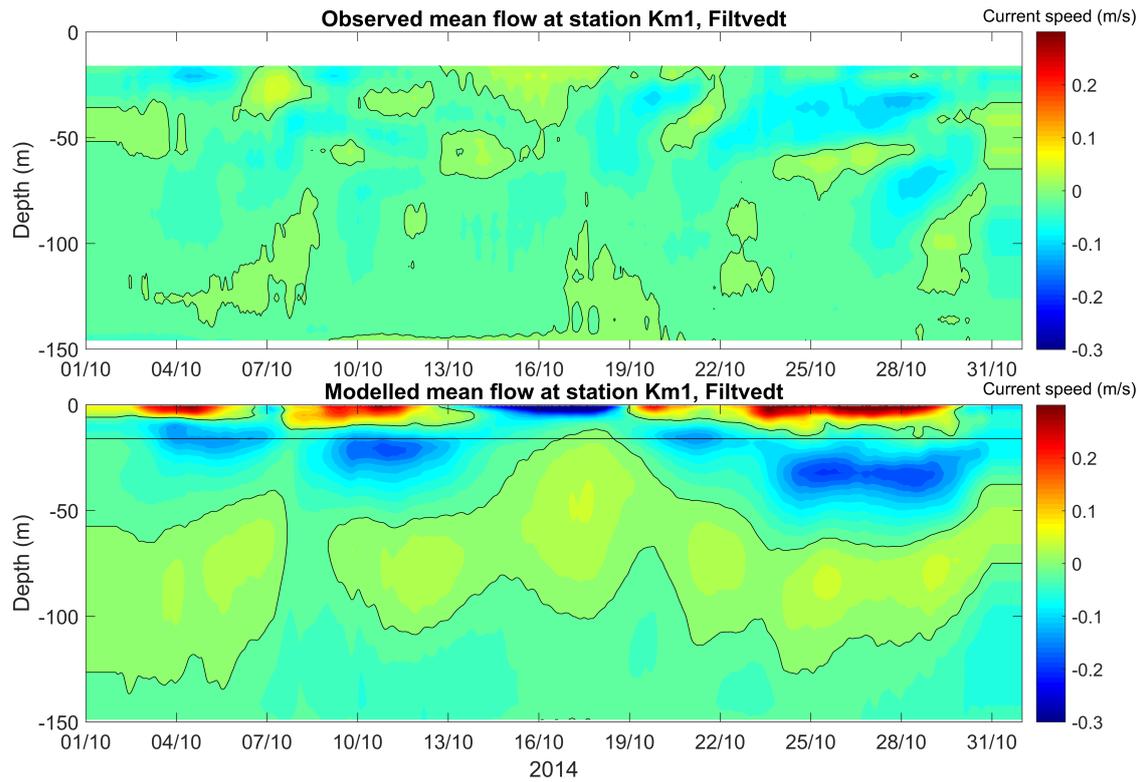
Figure 15: Observed (upper panel) and simulated (lower panel) mean currents from station Km1 (FB transect). The mean current is estimated by taking a running mean of 49 hours. The colorbar indicates the current speed in m/s along the channel. Red colors indicate flow into the fjord, while blue colors indicate flow out of the fjord. The black contourline shows where the mean flow is zero. The shallowest observations is at 16 m depth. This depth is indicated in the lower panel with a horizontal line.

Hjelmervik et al. (2017) used (1) to estimate the barotropic current at station Km1, and t_tide was used to find the tidal components. The results are shown in Table 4. The model performance for the semi diurnal components (S_2, M_2 and N_2) of the barotropic tides are very good. The amplitude of diurnal components (K_1 and O_1) are to weak and the phase is wrong. The model performance for the components with periods around 6 hours are relatively good.
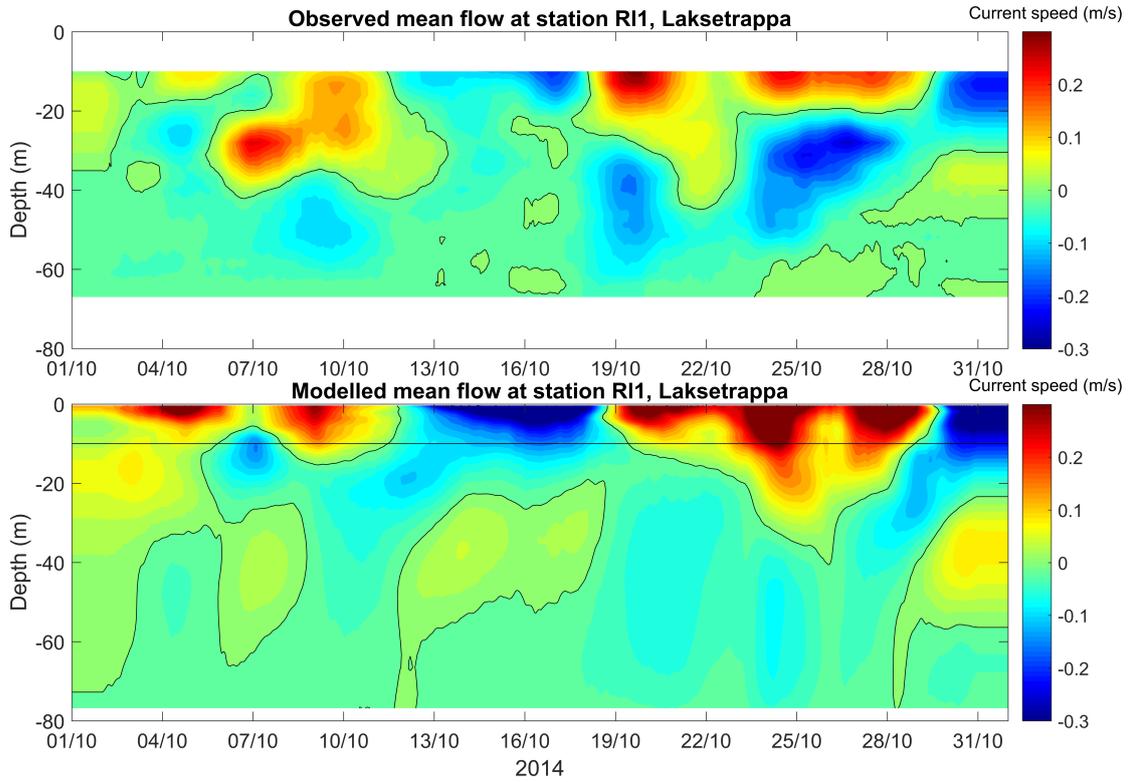
Figure 16: As Figure 15, but for Station Rl1 (SE transect) where the shallowest observation depth is at 10 m depth.

Table 4: Tidal major amplitudes (cm/s) and phases (deg) for the barotropic current at Km1.

Comp.	Period [h]	Observed [cm/s]	Observed [deg]	Simulated [cm/s]	Simulated [deg]
SS_2	12.0000	0.5	280	0.5	334
M_2	12.4206	1.8	9	2.0	16
N_2	12.6584	0.5	293	0.5	343
K_1	23.9345	0.5	61	0.0	261
O_1	25.8193	0.1	120	0.2	250
MN_4	6.2692	0.3	166	0.2	305
M_4	6.2103	0.7	220	0.7	290
MS_4	6.1033	0.0	252	0.4	19
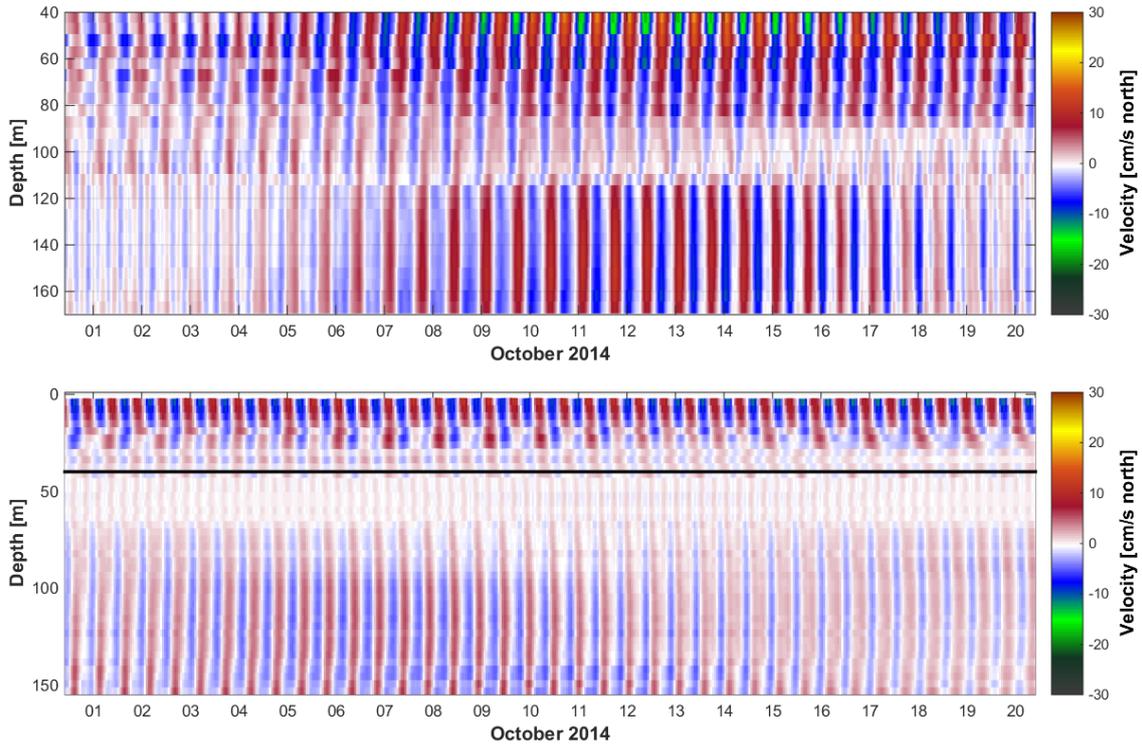
Figure 17: Extracted tides from the observations (upper panel) and the model results (lower panel) at station Km1. The colorbar indicates the current speed in m/s along the fjord. Red colors indicate flow into the fjord, and blue colors out of the fjord. The black contourline shows where the mean flow is zero. The shallowest observations is at 40 m depth. This depth is indicated in the lower panel with a horizontal line.

4.2.3 ExxonMobil mooring

The observed currents at Slagentangen are compared with simulated data at approximately the same location and depth (Figure 3).

Moving to the ExxonMobil mooring outside of Slagentangen we observe that the time series reveal, as shown by Figure 18, that the observed velocities varies and follows no striking pattern. The time series covers the period from 1st October 2014 until 30th November 2015. Current roses (Figure 19) reveal that both the observed and the simulated velocities are stronger in the upper layer, but that the simulated velocities are stronger than the observed velocities. The yearly maximum observed velocities are approximately 0.4 and 0.6 m/s at 10 and 2.5 meters depth respectively (Tab. 5). During 2014 and 2015 maximum observed velocity at 2.5 meters depth was 0.55 m/s in southeast direction (143^oN) the 26th of March 2014. The velocity at 10 meters depth was 0.08 m/s (153^oN) at the time of maximum velocity at 2.5 meters depth indicating that the velocities are different in the two layers, that is, baroclinic.
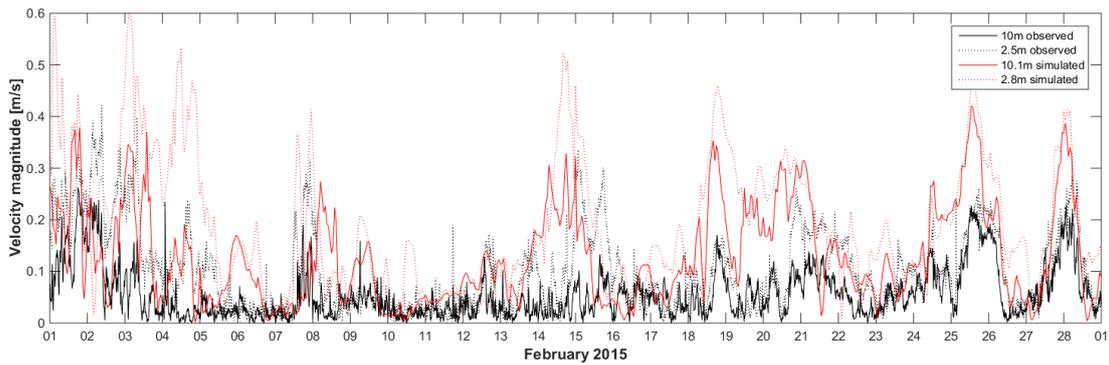
Figure 18: Timeseries of observed and simulated velocity magnitudes at Slagen.
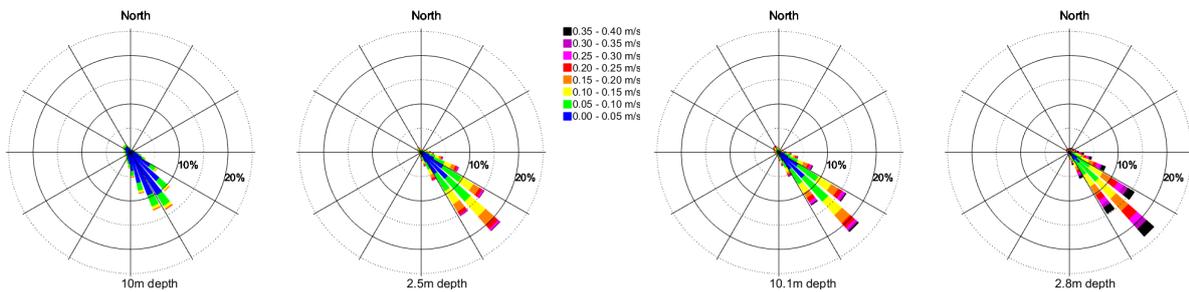
Figure 19: Current roses for observed (left) and simulated (right) velocity at the two depths from 1st of October 2014 to 1st of October 2015.

The mean directions are to the south east. At approximately 2.5 meters depth the mean directions are 146^oN and 139^oN for observed and simulated directions, respectively, which is in fairly

Table 5: Yearly maximum observed velocity at Slagen.

Year	Max. velocity at 10m depth			Max. velocity at 2.5m depth		
	Date	[m/s]	[deg]	Date	[m/s]	[deg]
2006	21 Jan 2006	0.42	139	31 Oct 2006	0.57	140
2007	14 Jan 2007	0.42	172	21 Aug 2007	1.03	359
2008	22 Mar 2008	0.36	149	19 Dec 2008	0.57	160
2009	17 Dec 2009	0.45	142	24 Mar 2009	0.56	139
2010	09 Nov 2010	0.41	138	09 Nov 2010	0.54	138
2011	01 Jan 2011	0.39	146	30 Mar 2011	0.62	185
2012	05 Dec 2012	0.39	138	29 May 2012	0.57	140
2013	10 Oct 2013	0.42	143	10 Oct 2013	0.49	144
2014	18 Apr 2014	0.44	147	26 Mar 2014	0.55	143
2015	24 Jan 2015	0.33	128	21 Mar 2015	0.55	141

good agreement. At approximately 10 meters depth the observed mean direction shifts to 170^oN while the simulated mean direction is 148^oN.

The probability density function (PDF) shown in Figure 20 first of all corroborates the finding of the previous paragraph that both the observed and the simulated velocities are stronger in the upper layer and that the simulated velocities are stronger than the observed velocities. The directional PDF reveals in addition that the model captures well the directions in the upper layer, but does not capture the change in direction between the two depths. The standard deviations at 2.5 and 10 meters are 55 and 66 degrees respectively for the observed directions, and 56 and 61 for the simulated directions, which is a fairly good agreement.

Finally the scatter plots reveal that the correlation in time is not satisfying (Figure 21). The model appears to have a problem in capturing the right phenomena influencing the currents at the right time. This is a well established fact and is not particular to the FjordOs model. All models of resolution high enough to capture the so called mesoscale and submesoscale activities (eddies, meaders and jet currents) is plagued by the same problem. The QQ-plot like the PDF plot confirms that the simulated currents are stronger than the observed currents.
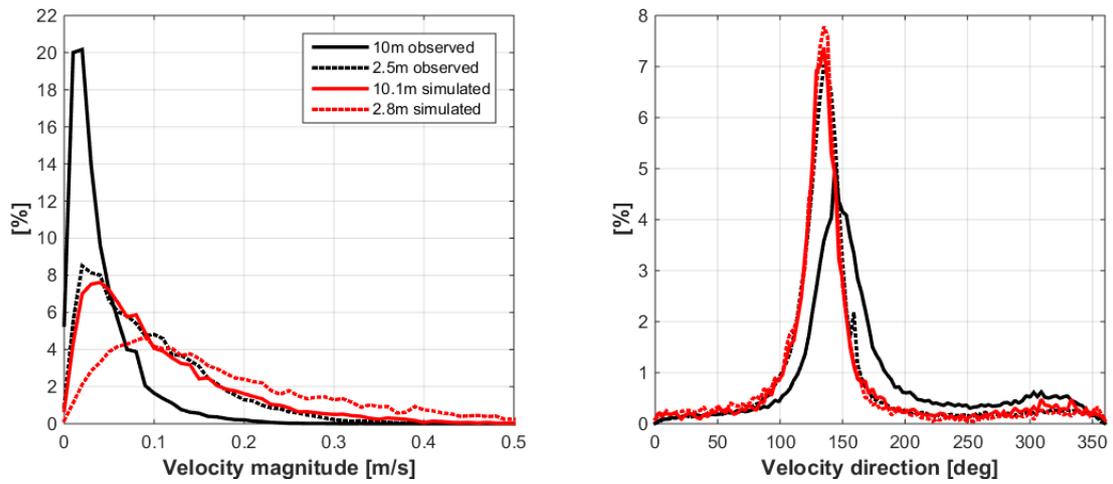
Figure 20: Probability density functions of velocities and directions at Slagen for 1st of October 2014 to 1st of October 2015. The bin width is 0.01 knots for velocity and 3 degrees for direction.
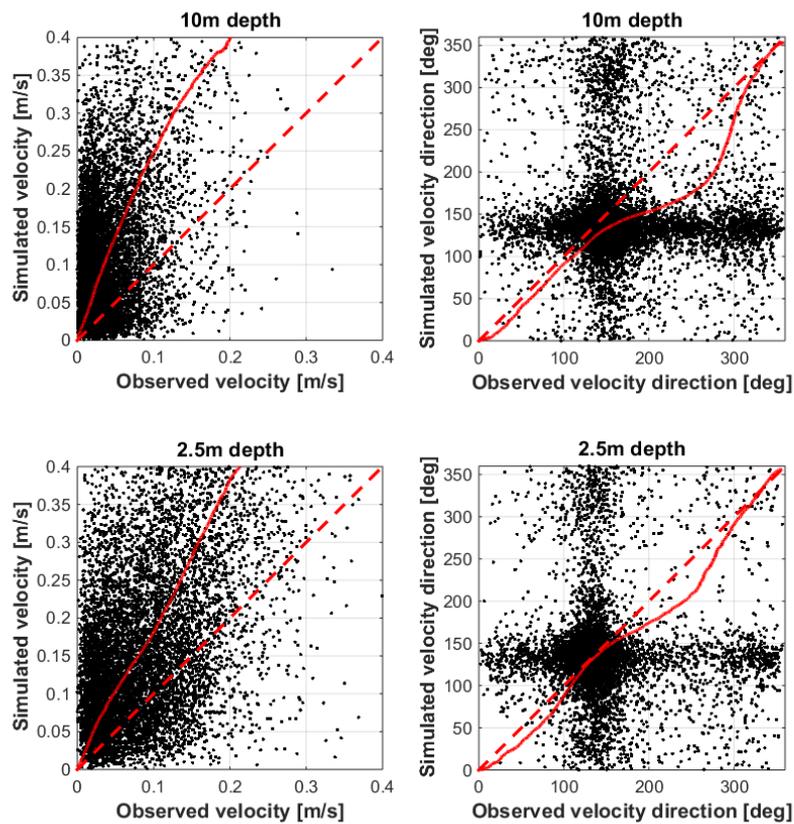
Figure 21: Combined qq and scatter plots of observed and simulated current at Slagen for the period 1st of October 2014 through 1st of October 2015.

28

4.3 CTD-measurements

4.3.1 Profiles of salinity and temperature

To evaluate the model's representation of the hydrography and stratification we have extracted temperature and salinity profiles from the model simulation at three of the CTD stations, namely OF-1, LA-1 and D-2. The locations of these three stations are shown by Figure 2 and listed by Table 2.

As revealed by Figures 22 through 24 the observations show in general that the upper layers are heated during the summer with maximum surface temperatures towards the end of the summer (August). This is also reflected in the simulations at all stations, but to a lesser degree. In addition the profiles in the outer parts of the fjord indicate that the upper layer is too thin in the simulated data. At larger depths, the water is too cold and the salinity is too high. This might indicate that the open boundary input and the representation of vertical mixing should be modified.
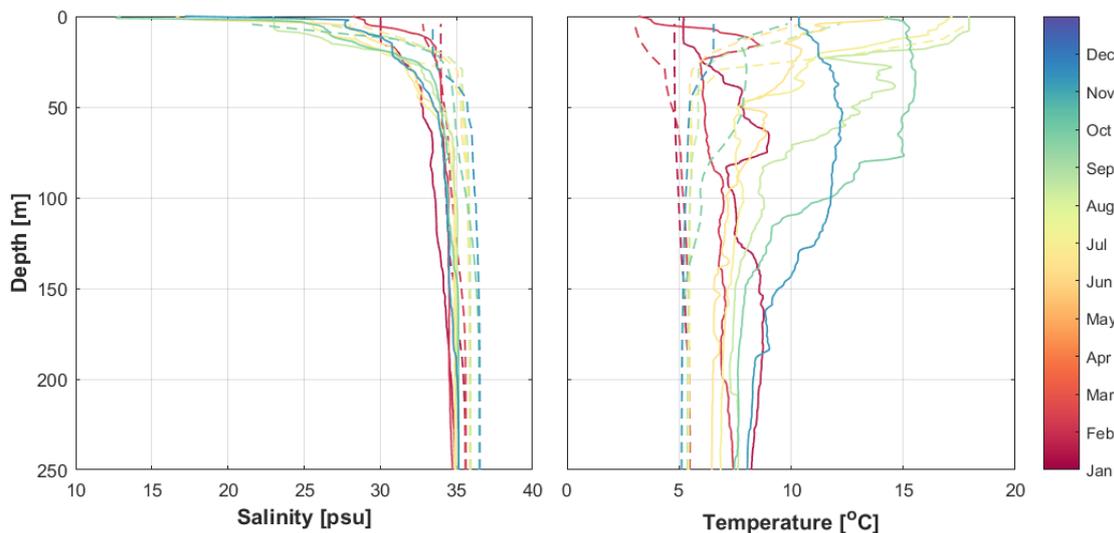
Figure 22: Observed (solid) and simulated (dashed) salinity and temperature profiles at station OF-1 Torbjørnskjær in the outer part of the Oslofjord. All profiles are from 2015.

The observations at LA-1 is taken in the Larviksfjord, which is on the western side of the Oslofjord and close to the southern open boundary of the FjordOs model. In such shallow waters the observations reveal that the whole water column is heated during summer and cooled during winter. In contrast the simulated temperature profile varies only in the upper 20 meters (Figure 23).

The third CTD station chosen (D-3) is inside of the Svelvik Sill in the Drammensfjord (Figure 24). The water masses below sill depth in the Drammensfjord are known to be stagnant over longer periods and hence to become nearly anoxic. The reason is probably the same as explained
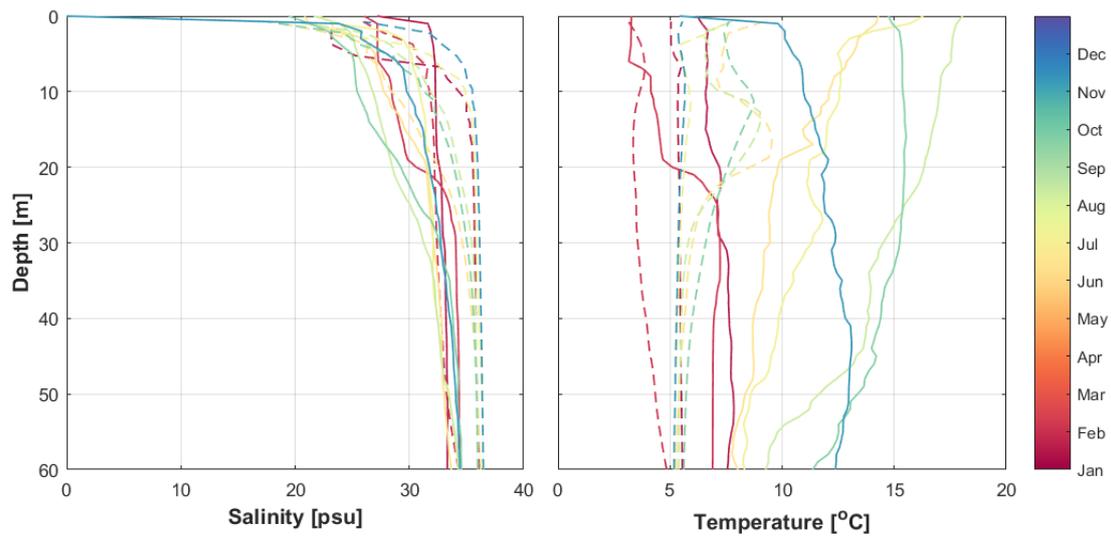
Figure 23: Observed (solid) and simulated (dashed) salinity and temperature profiles at station LA-1 Larviksfjord in a fjord branch in the outer part of the Oslofjord. All profiles are from 2015.

in *Staalstrøm and Røed* (2016), that is, a too weak vertical mixing below sill depth obstructing frequent deep water renewals. In contrast the simulated profiles reveals that below sill depth the salinity is much lower and the temperature somewhat higher than what is observed leading to a water mass that is much lighter. Following *Staalstrøm and Røed* (2016) this can only be explained by postulating that the vertical mixing in the model is too high.
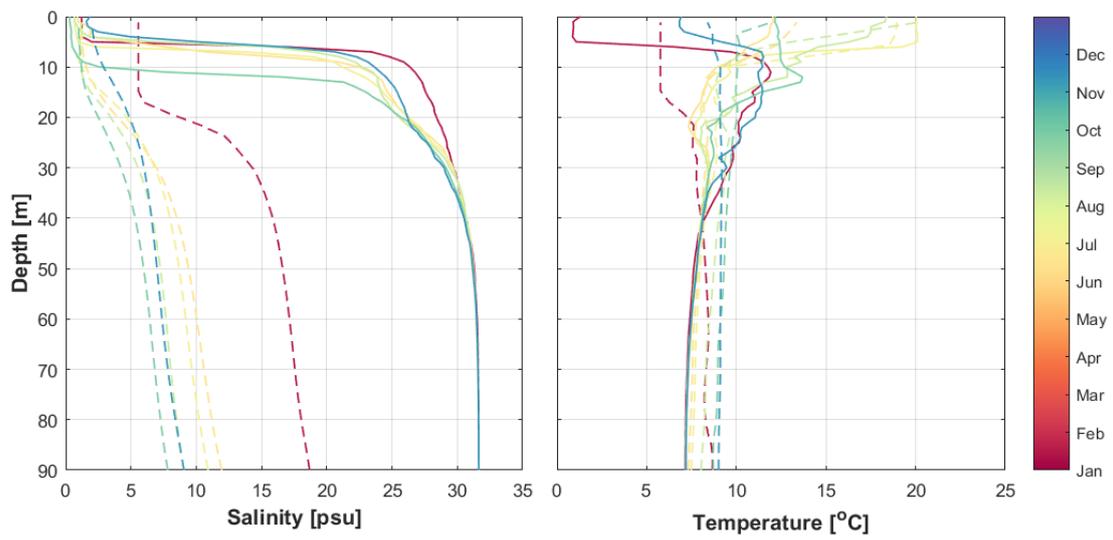
Figure 24: Observed (solid) and simulated (dashed) salinity and temperature profiles at station D-3 Solumstrand. All profiles are from 2015.

4.3.2 Time evolution of salinity and temperature

To assess how the model simulates the time evolution of the water masses properties we have chosen to plot so called Hovmøller diagrams of the observed and simulated salinities and temperatures at the three stations D-3, OF-5 and OF-1 (). Note that Station OF-5 is in the middle of Breidangen.

Comparing the *observed* salinity at stations OF-5 and OF-1, as shown by Figures. 25 and 26, we notice that the variations at for instance at 40 m depth at OF-5 follow the variations at OF-1, but is approximately 1 psu fresher. This indicate a relatively good water exchange in the outer part of the fjord system. The water masses below sill depth at D-3 in the Drammensjord is different. The salinity below 40 m depth is lower than at the same depth in Breidangen and changes very little in time. These in support of the hypothesis that the water masses inside of the sill and below sill depth (12 m) in the Drammensfjord is more or less stagnant. This is in contrast to Stations OF-5 and OF-1 where the seasonal temperature changes in the surface layer is diffused down in the water masses (middle and lower panel of Figure 26). The temperature at 100 m depth has a seasonal change, but the maximum value is shifted in time, so the highest temperatures are found in the start of January at this depth.

Regarding the *simulated* water mass properties we notice, as shown by Figures 27 and 28, that the water exchange in the model between the two stations OF-5 and OF-1 is relatively good. We also notice that the variations at OF-5 follow the variations at OF-1 as for the observations. The modelled salinity however is to high at mid depth compared to the observations. This may be due to wrong open boundary input or too weak vertical mixing. The upper panel in Figure 27 shows that the deep water masses in the Drammensfjord (D-3) have a high salinity at model initialisation, but that fresh water from the surface is quickly mixed down.

Finally we note that when the modelled temperature evolution at OF-1 is compared with the observations, the vertical mixing seems to be too low, and the heating of the surface water during summer do not penetrate deep enough during the winter. While inside the Svelvik Sill (D-3) the surface waters are mixed down too deep. Thus the vertical mixing appears to be too weak in the open part of the fjord, while being too vigorous inside the sills.
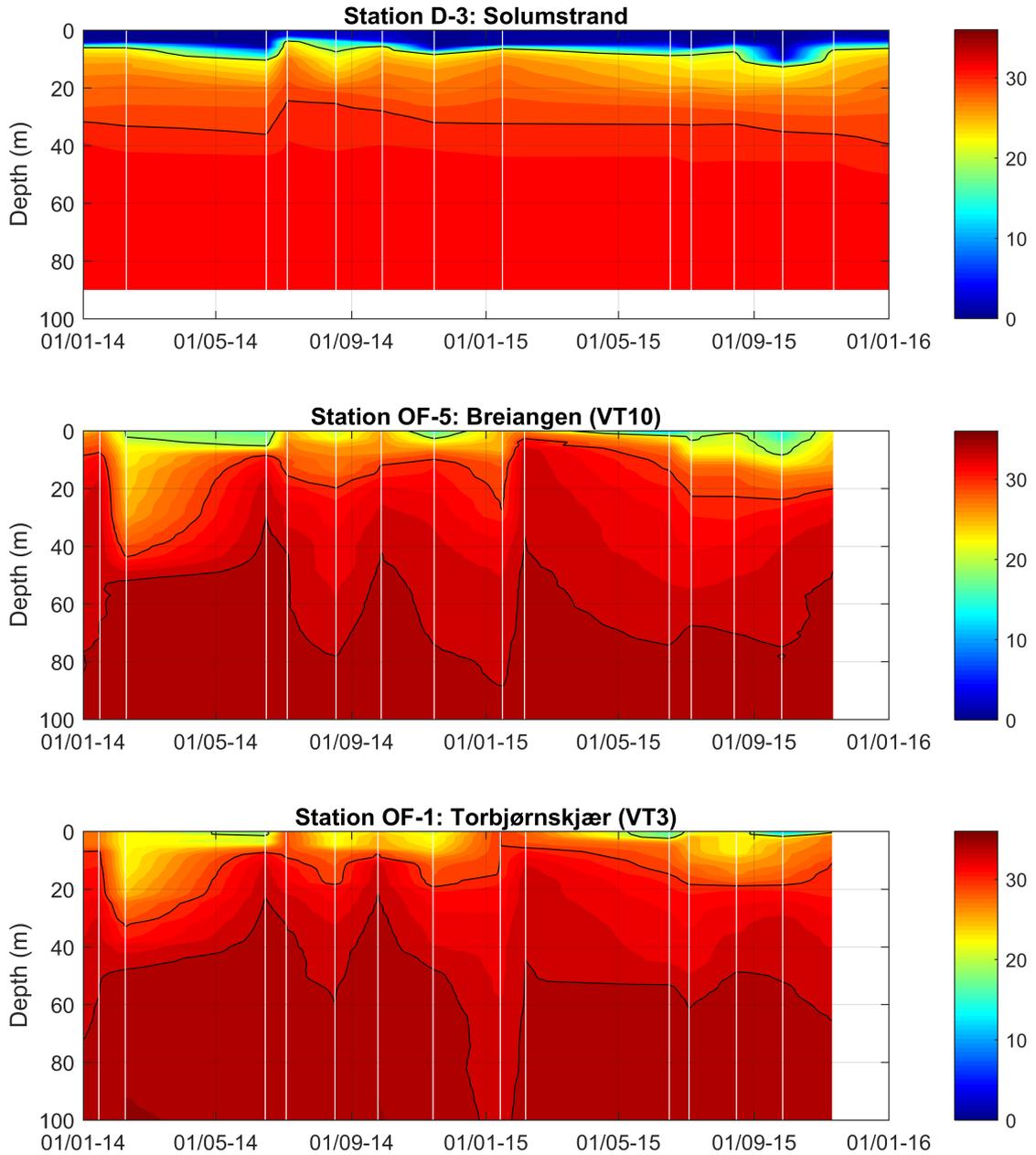
Figure 25: Observed salinity at three stations in the Oslofjord. Contour lines mark 20, 30, and 34 psu. The white vertical lines indicate the positions when CTD casts were taken.
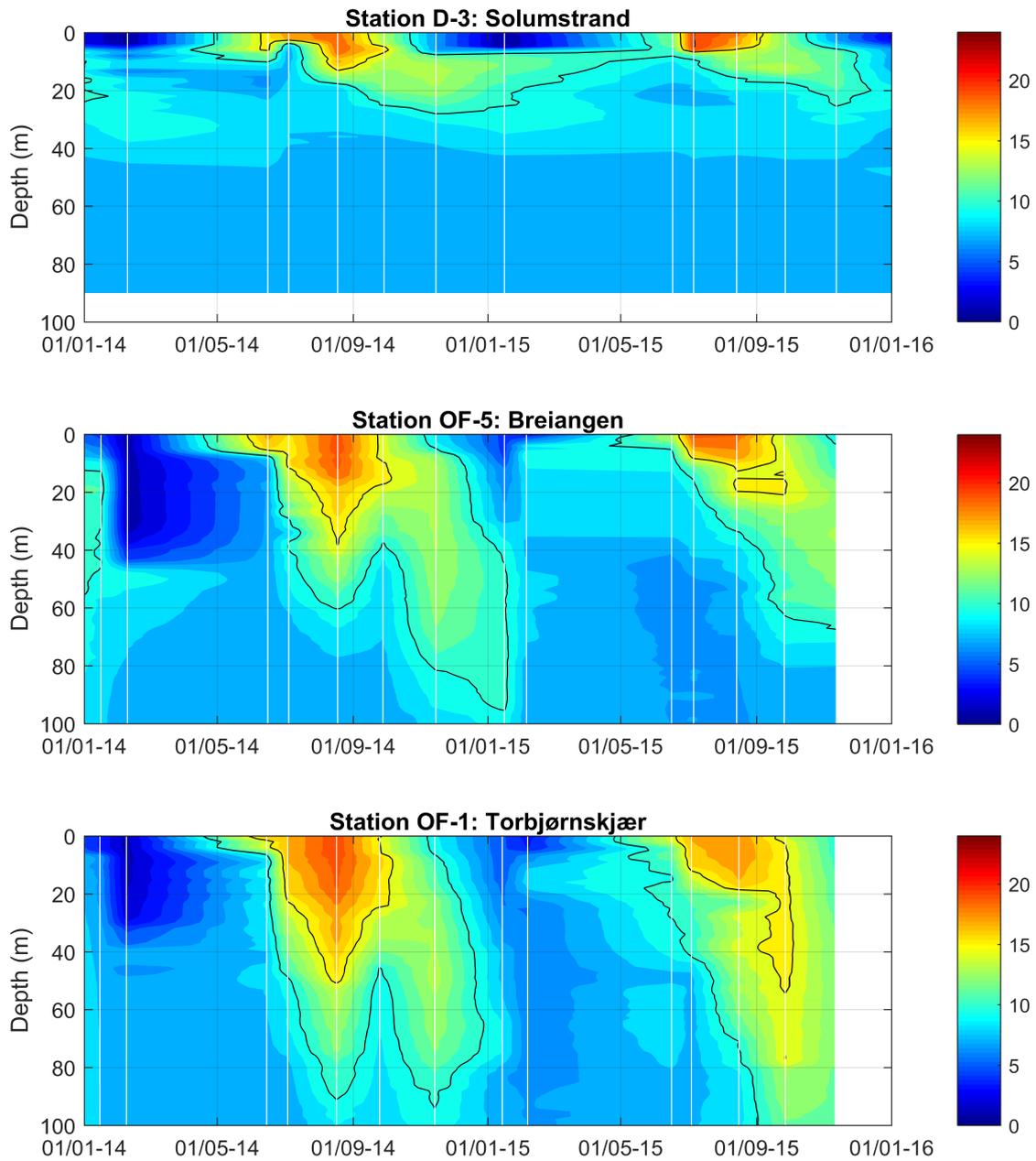
Figure 26: Observed temperature at three stations in the Oslofjord. Contour lines mark 5 and 10 ^{o} C. The white vertical lines indicate the positions when CTD casts were taken.
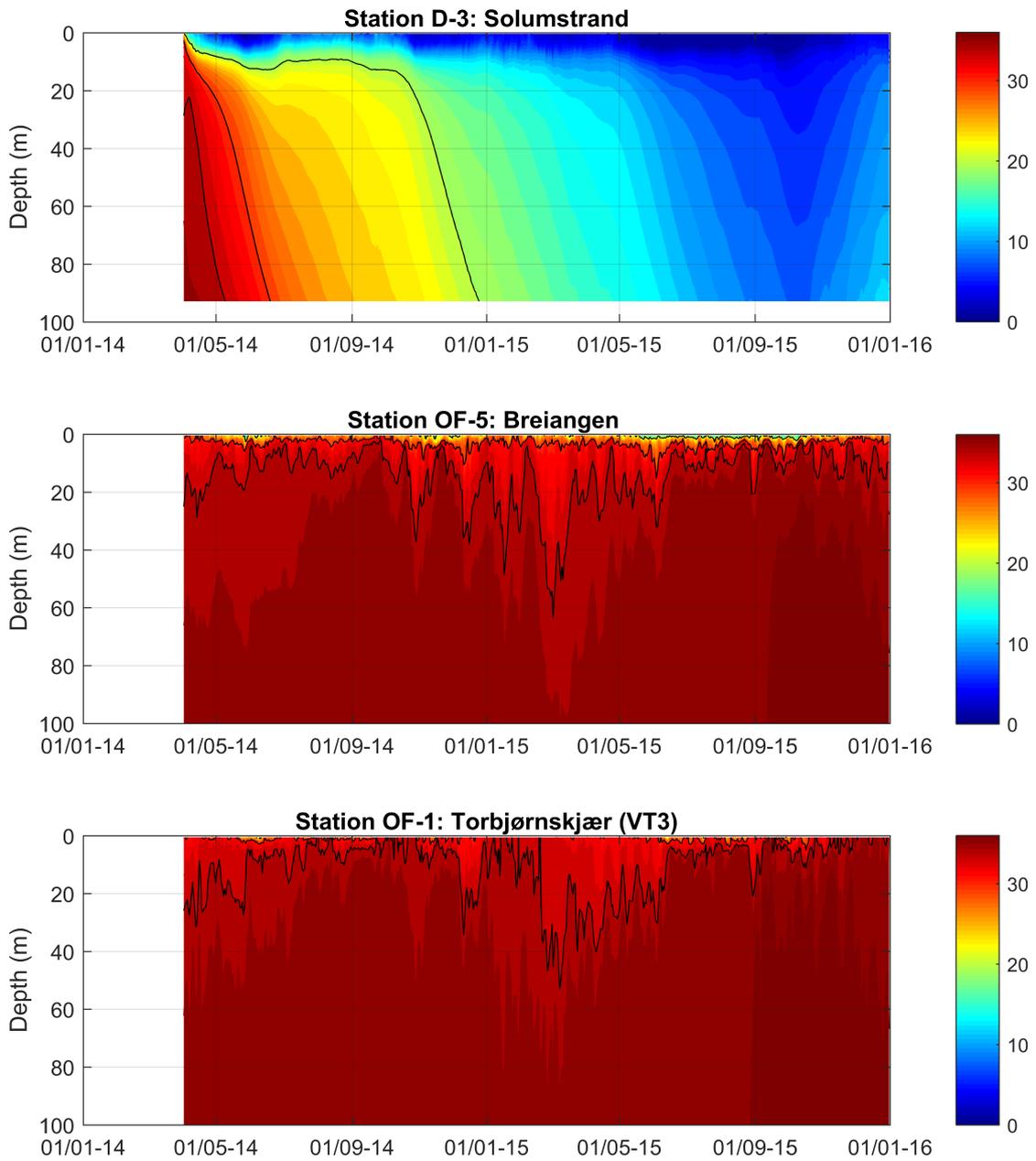
Figure 27: Modelled salinity at three stations in the Oslofjord. Contour lines mark 20, 30, and 34 psu.
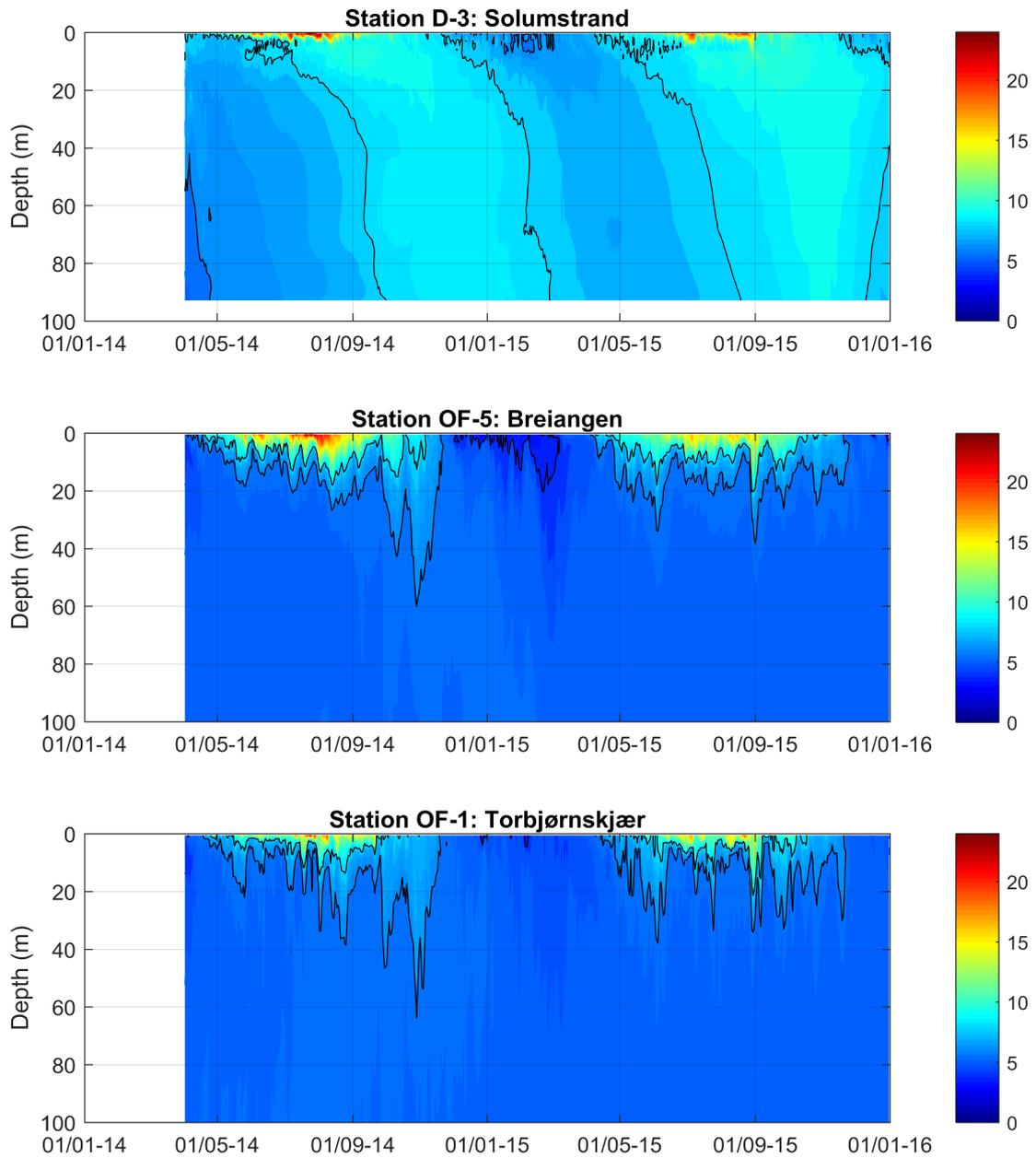
Figure 28: Modelled temperature at three stations in the Oslofjord. Contour lines mark 5 and 10 °C.

4.4 Temperature measurements

4.4.1 The Scanmar mooring

The temperature observations from Scanmar AS are compared with simulated data extracted from 1.15 meters depth at approximately the same location as the observations. The time series shown by Figure 29 reveal that the simulated and observed temperature are in fairly good agreement, in particular during winter and spring. In the summer and fall the model underestimates the temperature with a few degrees. This is underscored by the combined qq and scatter plots shown by Figure 30). Finally, as is evident in the zoomed time series shown by the lower panel of Figure 29, the model captures the timing of the daily variations in temperature well, but appears to overestimate the heating and cooling. The latter is probably caused by too large daily variations in the forcing.

2014 had a warmer summer than 2015. This is evident in both the observations and the simulations (Tab. 6). The summer months of 2014 also had the largest variance in both the observed and the simulated temperature during 2014 and 2015. Generally, the simulated monthly temperature had a larger variance than the observed monthly temperature. The mean of the observed and simulated temperatures are 10.0^oC and 8.6^oC respectively, while the variances are 27.2^oC and 21.1^oC respectively.

Table 6: Monthly statistics for observed and simulated temperature at Åsgårdstrand.

		2014			2015		
		quantity	mean	variance	quantity	mean	variance
Jan	obs	558	2.5	6.2	558	4.9	2.5
	sim	745	-	-	745	4.0	0.7
Feb	obs	504	1.8	0.5	504	4.0	1.8
	sim	673	-	-	673	3.6	0.6
Mar	obs	496	3.7	0.6	496	4.2	0.4
	sim	745	-	-	745	4.7	0.3
Apr	obs	515	7.5	4.1	515	7.0	2.1
	sim	721	7.6	7.1	721	7.4	2.8
May	obs	544	12.1	9.3	544	10.3	1.3
	sim	745	11.3	10.4	745	9.9	3.5
Jun	obs	531	16.2	4.2	531	14.0	3.9
	sim	721	15.5	8.3	721	12.8	6.0
Jul	obs	558	20.2	10.5	558	17.1	2.0
	sim	745	17.0	24.3	745	14.6	5.1
Aug	obs	512	20.0	3.2	512	18.2	1.3
	sim	745	16.4	5.6	745	15.5	8.7
Sep	obs	536	16.3	1.9	536	15.1	1.2
	sim	721	12.9	8.9	721	12.7	2.5
Oct	obs	557	12.3	1.7	557	10.6	0.8
	sim	745	9.0	1.5	745	8.6	2.7
Nov	obs	540	8.3	2.9	540	8.8	2.4
	sim	721	6.3	2.0	721	6.1	1.3
Dec	obs	490	4.4	3.6	490	7.8	0.4
	sim	733	3.4	1.5	733	4.8	0.8
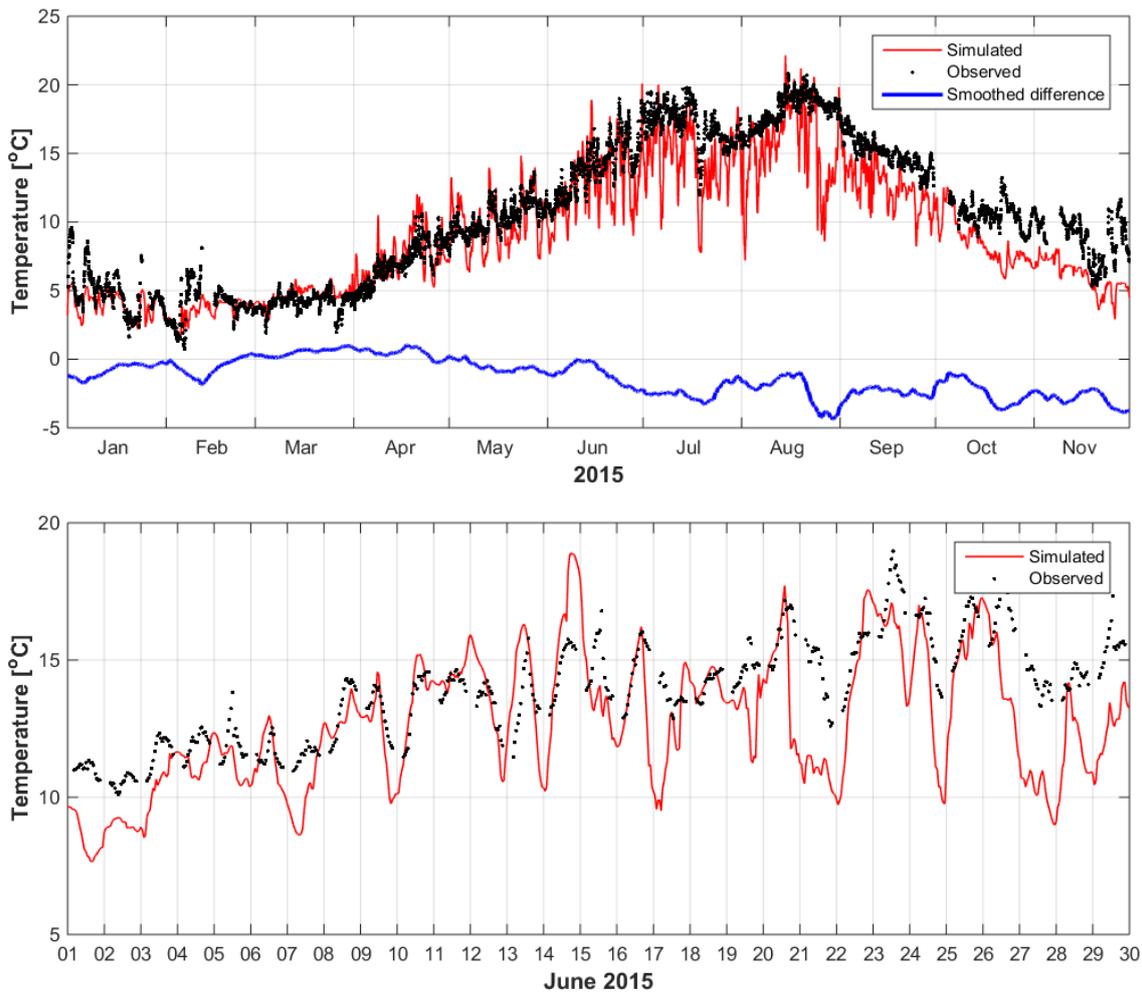
Figure 29: Time series of observed and simulated temperatures at the location and depth of the Scanmar mooring off Åsgårdstrand. Upper panel is for the year 2015 while the lower panel is a zoom in on the month of June 2015. Black dots refer to the observations, while the solid red curve is the simulated temperature record. The solid blue line in the upper panel is the difference between the two smoothed over 10 days.
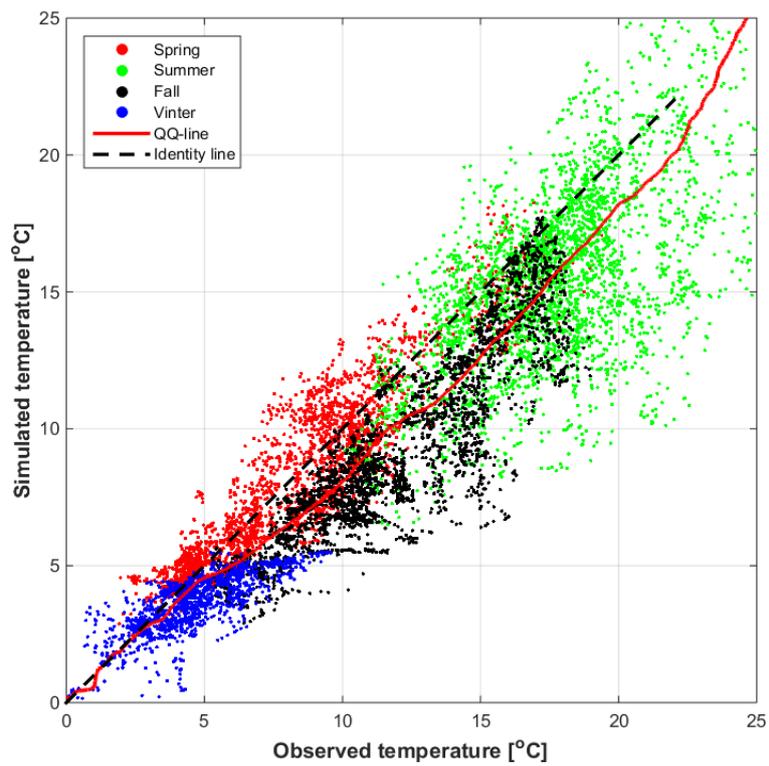
Figure 30: Combined QQ- and scatter plot of observed and simulated temperatures at the location and depth of the Scanmar mooring off Åsgårdstrand.

4.4.2 Temperatures in the Inner Oslofjord

We now turn our attention to the observed and simulated temperatures at the three beaches in the Inner Oslofjordt. Since the temperatures are observed close to the shoreline only 40 cm under the surface and near some river outlets, the temperature is heavily influenced by the weather conditions and the local circulation patterns. The model is therefore not expected to capture such detailed effects. Nevertheless, as revealed by Figures 31, observations and modelled results are in relatively good agreement both in temperature level and in the fluctuations.

The temperature differences during the day are larger in the model than in the observations. The observed temperature increases 1-3 degrees from 09:00 to 18:00 and is not measured during the night, while the modelled temperature increases up to six degrees from 06:00 to 23:00. The fact that temperature is not measured during the night, but only from 09:00 to 18:00, might explain differences i temperature rise during the day, but the difference might indicate too much heating in the model.

During the summer 2014 the model predicts higher temperatures at Sjøstrand than was observed. The observations in Hvalstrand have some of the same trends as the modelled temperature with temperatures up to 25 degrees. The air temperatures in 2014 was higher than in 2015 and resulted in higher water temperatures, especially in shallow areas.

Figure 31: The observed and modelled temperature at three beaches in the Inner Oslofjord during the summer of 2014 (three upper panels) and summer of 2015 (three lower panels

42

4.5 The Godafoss oil spill

Unfortunately there is no overlap between the time period covered by the FjordOs hindcast and the time when the container ship Godafoss ran aground. So no direct comparison between simulated oil drift based on input from the FjordOs model is possible as part of this evaluat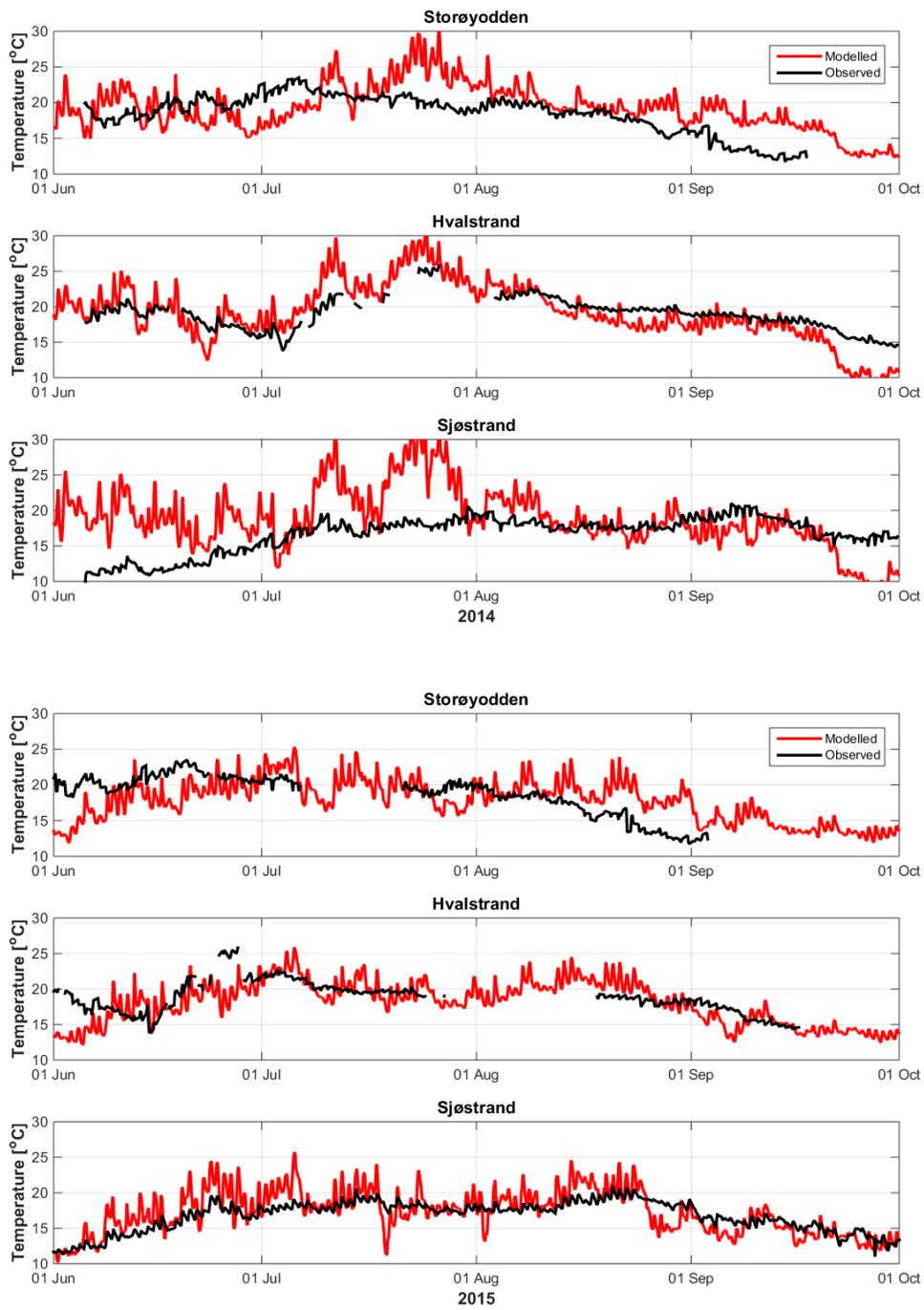ion. Nevertheless, to investigate whether the FjordOs model provides results that are similar to the data gathered during the Godafoss oil spill (Section 3.5), we have opted to map the pathway of a feigned oil spill. To this end we have released Lagrangian particles for a time period of one year (April 1st 2015 to April 1st 2016) at the location where the Godafoss grounded, and simulated particle trajectories using the open source trajectory-model OpenDrift[2]. We argue that over such a long period of time, there will be at least one situation similar to the weather and currents experienced during the Godafoss release.

The OpenDrift model was forced with currents from the FjordOs model and with winds from the Arome-MetCoOp 2.5km (Arome2.5) atmospheric model (*Müller et al.*, 2017). The latter is the same atmospheric model we used as forcing when running the FjordOs hindcast. To properly treat the particles that are advected out of the FjordOs-model domain, and to enable them to re-enter at the correct location, we provided daily mean currents from NorKyst-800m outside of the FjordOs-model domain.

There are a number of parameters that may be tuned when running OpenDrift. One such parameter is the wind drift factor, which we set to 0.01 (i.e. 1%). Otherwise we used the default parameter values. Particles are released once per hour throughout the one year simulation for a total of 8760 particles. The lifetime of each particle is set to 15 days, that is, after 15 days the particle is deactivated. This is done to reduce the computational cost of advecting a large number of particles. We further divided our area into a rectangular cells, and measured the number of hours from the particles were released until they reached the different cells. In addition we counted the number of particles that had been inside each cell during the simulation. The latter gives insight into the probability of experience oil in the individual cells. The size of the cells were chosen to be 140 x 140 meters, a balance between having too small or too large cells. If too small we might end up having too few particles in some cells, or if too large too many particles ends up in the same cell. The results are presented by Figures 32 through 34.

Comparing the results to the observed oil displayed by Figure 5, we observe that there are some obvious similarities between the observations and the simulations. For instance the right-hand panel of Figure 34 shows, in similarity with the observations, that a substantial number of

---

[2]OpenDrift is distributed under a GPL v2.0 license, and is available on GitHub (https://github.com/knutfrode/opendrift). This is a trajectory model under development at MET Norway, and is described by its developers as "a software for modelling the trajectories and fate of objects or substances drifting in the ocean, or even in the atmosphere".
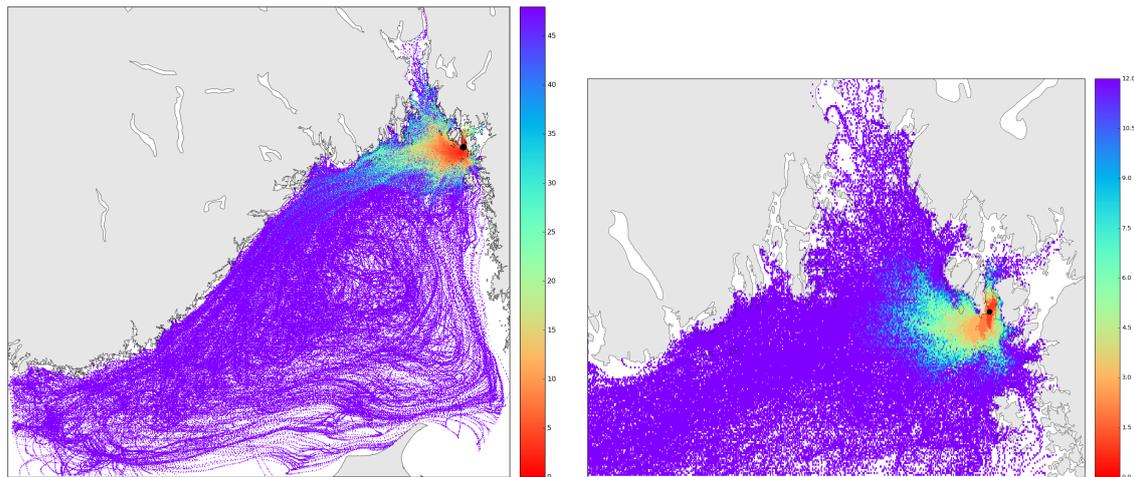
Figure 32: Displayed is the time it takes a Lagrangian particle to reach inside a given 140 x 140 m area after it is released based on a one year simulation. The location of the release is marked by a black solid circle, and corresponds to the location where Godafoss ran aground. The color bar indicates the time in hours. Left-hand panel shows the time up to and including 47.5 hours, while the right-hand panel shows the time up to and including 12 hrs and for a smaller domain.

particles are transported westward from the release position and strand along the Vestfold coast, the islands around Tjøme, and the Færder lighthouse. We also note the very low number of particles that strand at the peninsula west of Stavern (the area far left in Figure 34). This corresponds well with where the oil was observed or not. Looking at the left-hand panel of Figure 34 we would like to draw attention to two areas, namely Stavern and Bustein located, respectively, in the far lower left and the middle of Figure 34. As displayed by Figure 34 the feigned oil strands at Bustein after approximately two days, while at Stavern (Korntin) the oil strands after about four to five days. These stranding times corresponds well with the timing shown by Figure 5.
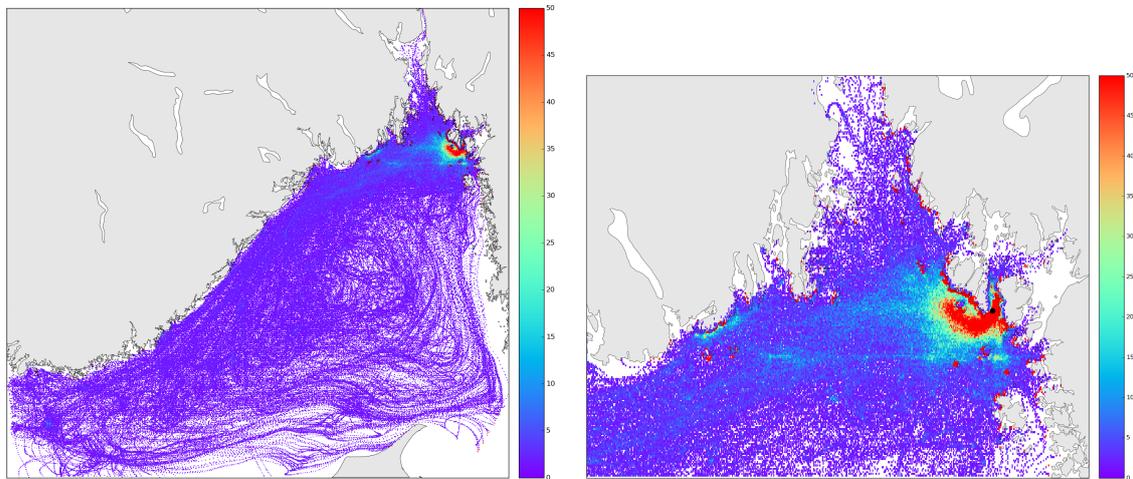
Figure 33: As Figure 32, but showing the number of particles that has been inside a given 140x140 m area during the simulation. The colourbar indicates number of particles from 0 (blue) to 50 (red). Right-hand panel is a zoom in of the left-hand panel.
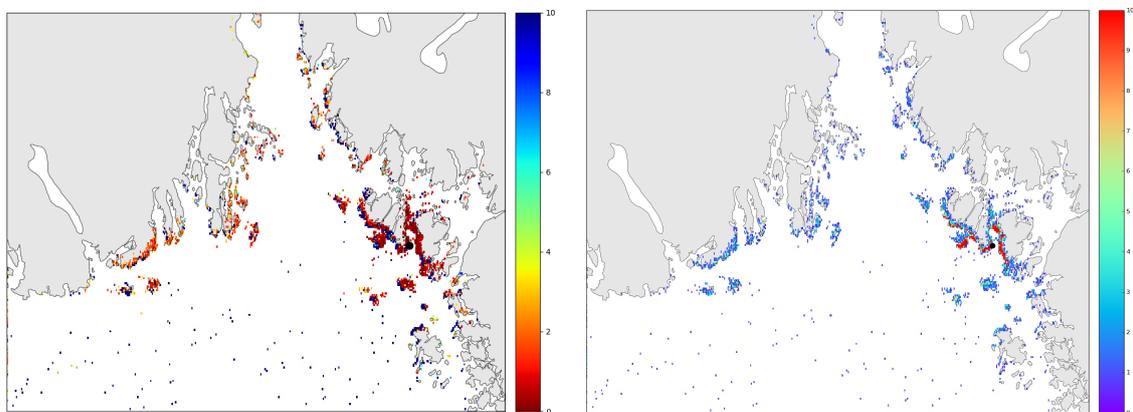
Figure 34: As Figures 32 (left-hand panel) and 33 (right-hand panel), but showing only the end position of each particle trajectory. The colourbar attached to the left-hand panel indicates the number of *days* ranging from 0 (red) to 10 (blue) it takes a particle to reach a given cell of size 140 x 140 meter, while the colourbar attached to the right-hand panel indicates the number of particles ranging from 0 (blue) to 10 (red) that has been inside a given cell of size 140 x 140 meter.

4.6 Surface drifters

We evaluate the models ability to recreate the drifter trajectories by using a skill-score developed by *Liu and Weisberg* (2011). It is defined by

$$ss = \begin{cases} 1 - \frac{s}{n} & ; \quad s \leq n \\ 1 & ; \quad s > n \end{cases}, \quad \text{where} \quad s = \sum_{i=1}^{N} d_i / \sum_{i=1}^{N} l_{oi}. \tag{4}$$

Here N is the total number of time steps, d_i the distance between the modelled and observed endpoints of the Lagrangian trajectories at time step i after the release, l_{oi} the length of the observed trajectory at time step i, and n a tolerance threshold. Thus if $ss = 1$ it implies a perfect match while $ss = 0$ means no skill. To investigate the skill of the FjordOs model we released Lagrangian particles into OpenDrift and computed the skill-score for each of the 15 drifters released as part of the FjordOs project (Section 3.6) using the FjordOs hindcast as input. Furthermore, to investigate whether the FjordOs model has a better skill than a coarser resolution model we also computed the skill-score using the NorKyst800 model results as input. In computing the skill-score we used a tolerance threshold $n = 2$ to get positive values for most trajectories.

Drop no.	Full trajectory		First hour only	
	FjordOs	NorKyst-800	FjordOs	NorKyst-800
1	0.77 (11)	0.68 (11)	0.17	0.14
4	0.78 (2)	0.53 (1)	0.55	0.45
6	0.00 (3)	0.84 (11)	0.07	0.46
8	0.82 (21)	0.58 (21)	0.00	0.00
51	0.58 (3)	0.73 (15)	0.49	0.58
52	0.38 (4)	0.50 (1)	0.37	0.47
61	0.58 (3)	0.70 (8)	0.49	0.58
91	0.51 (8)	0.50 (12)	0.73	0.67
101	0.61 (15)	0.78 (15)	0.63	0.78
102	0.59 (6)	0.75 (7)	0.87	0.77
Avg.	**0.56**	**0.66**	**0.43**	**0.49**

Table 7: Skill-score of drifter trajectories released during the September 2015 cruise. The numbers in parenthesis in column two and three indicate how many hours we were able to follow each model trajectory. The last two columns reveal the skill-scores following each trajectory for the first hour only.

Regarding the 13 drifters released in September 2015 we used both wind and currents as input. Note that the wind input used in OpenDrift is the same as the one we used to force both FjordOs and NorKyst800. The resulting skill-scores for 10 out of the 13 drifters are presented by Table 7, while the trajectories are displayed by Figures 35 - 38. The rationale for limiting the number of drifters to 10 is that some of them stranded too soon after the release to compute a meaningful skill-score.

As revealed by Table 7 we observe that the *average* NorKyst-800 skill-scores are higher compared to FjordOs. This is also true when we consider the *average* skill-score of the first hour of the trajectories. Nevertheless we notice that FjordOs has a higher skill-score for some of the full trajectories, e.g., drop nos. 1, 2, and 8, and also for the 1 hour trajecories, e.g., 1, 2, 91, and 102. Furthermore by performing a visual comparison between the trajectories (Figures 35 - 38) we are tempted to conclude that the trajectories based on the FjordOs model more often compares well to the observed trajectories than those based on NorKyst-800. We leave this up to the reader to decide. We merely state that the skill-scores alone appear to be insufficient to make a conclusive statement.
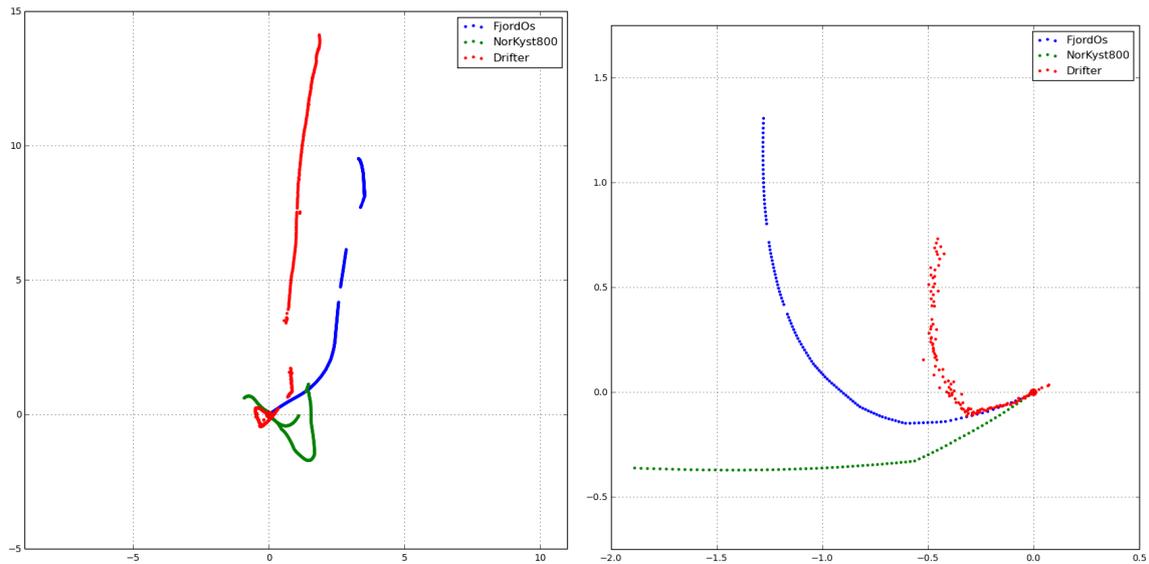
Figure 35: Displayed are modelled and observed drifter trajectories September 2015. The colours indicate trajectories based on NorKyst-800 (green), FjordOs (blue), and observed (red). Dotted lines form a grid of equal distances with origo at the release point. Drop 1 is to the left (5 km grid), while drop 4 is to the right (0.5 km).

Regarding the two drifters released in September 2014 we only used current as input. The resulting skill-scores are presented by Tables 8 and 9, while Figures 39 and 40 displays the modelled and observed trajectories. As revealed the FjordOs model performs better than the NorKyst-800,

but there is a clear weakness here since hourly data from NorKyst-800 is not available. Also, there are only two drifters. We observe that the FjordOs model has the highest skill-score based on both hourly and daily average data, and was the only model to transport the drifters as far south as the observed drift.

Drop no.	FjordOs 1h	NorKyst-800m 24h
1	0.79 (15)	0.73 (15)
2	0.84 (19)	0.76 (19)
Avg.	**0.81**	**0.75**

Table 8: As Table 7, but for the drifter release during the September 2014 cruise. Note that the FjordOs data are based on hourly resolution as input, while the NorKyst-800 data are based on daily averages.

Drop no.	FjordOs 24h	NorKyst-800m 24h
1	0.85 (15)	0.73 (15)
2	0.91 (19)	0.76 (19)
Avg.	**0.88**	**0.75**

Table 9: As Table 8, but modelled trajectories from FjordOs are based on daily average ocean currents to get a more fair comparison between the models.

We conclude that none of the models gives a perfect match, and that the currents in NorKyst-800 appears to be too weak during these drifter releases. Furthermore we think it is safe to conclude that the FjordOs model provides a better skill overall. It should be kept in mind though that, given the low number of drifters and their limited spatial and temporal distribution, more drifter studies should be performed in which the released drifters should have a better temporal and spatial distribution. In particular it would be interesting to release drifters in some of the narrow straits and sounds, and in the Archipelagoes.
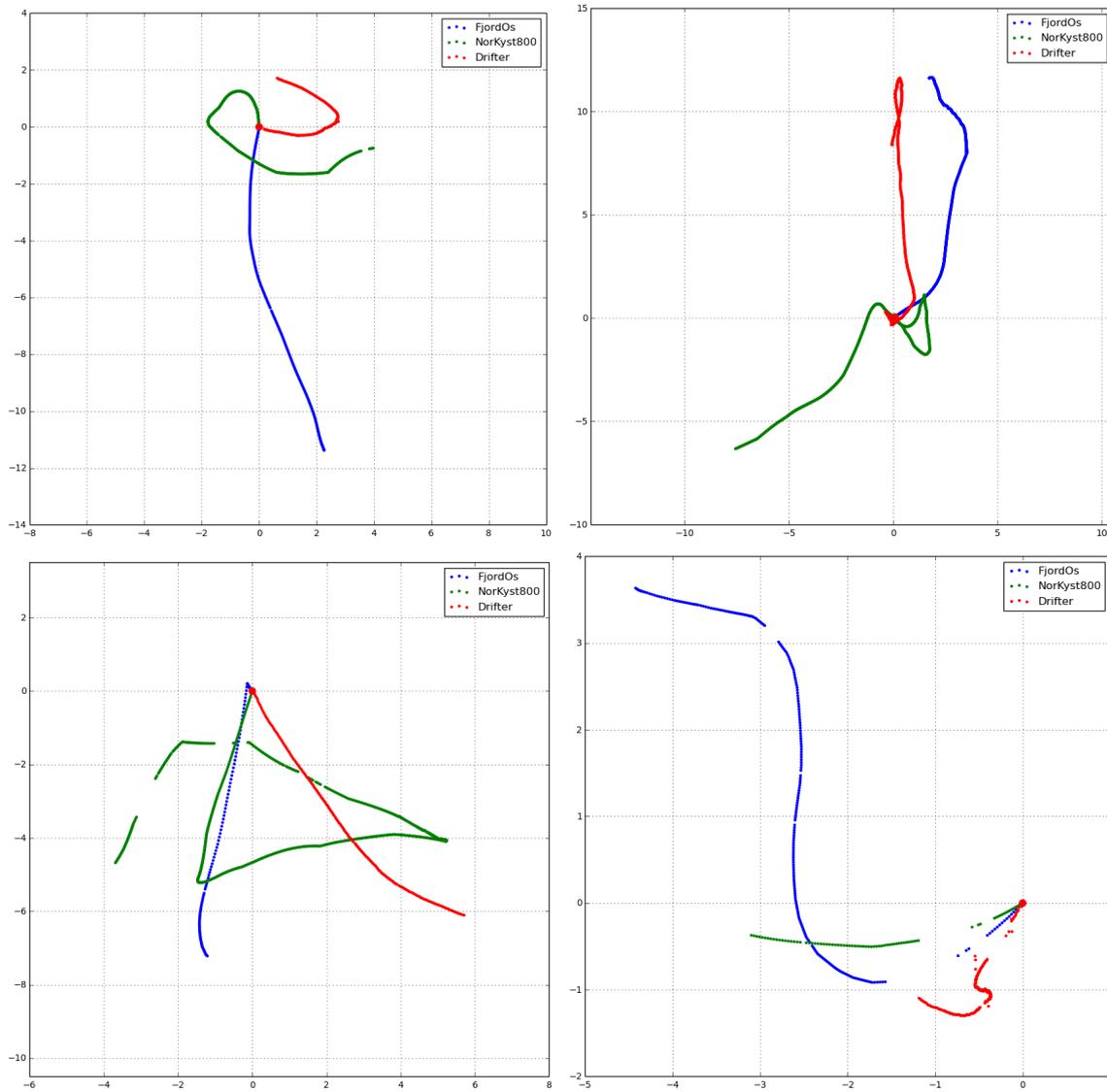
Figure 36: As Figure 35, but showing drop 6 (top left, 2 km grid), and drop 8 (top right, 5 km grid), drop 51 (bottom left, 2 km grid) and drop 52 (bottom right, 1 km grid).
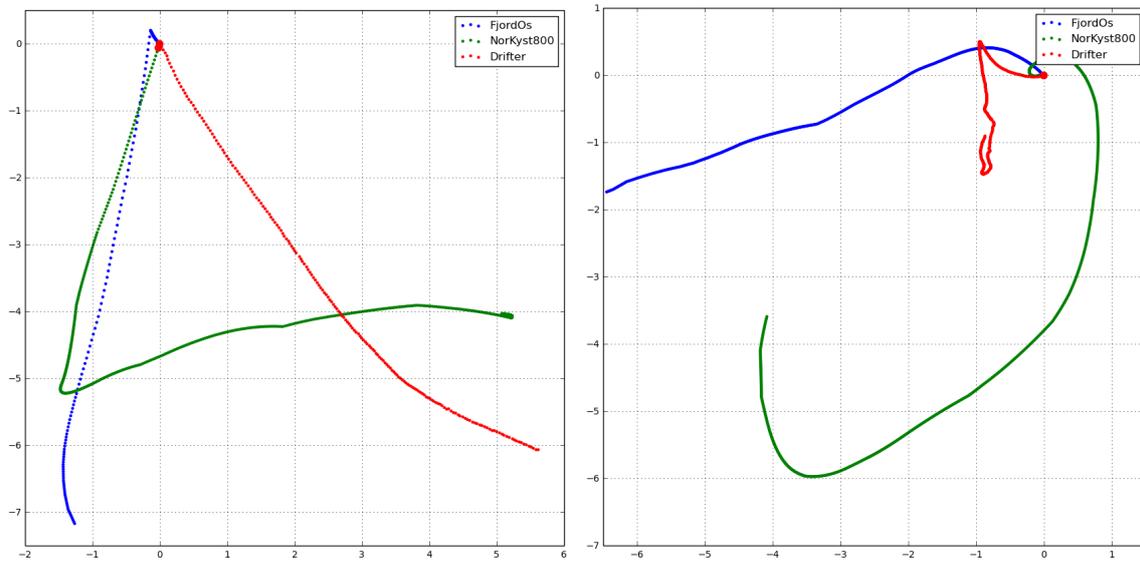
Figure 37: As Figure 35, but showing drop 61 (lef-hand panel, 1 km grid) and drop 91 (right-hand panel, 1 km grid).
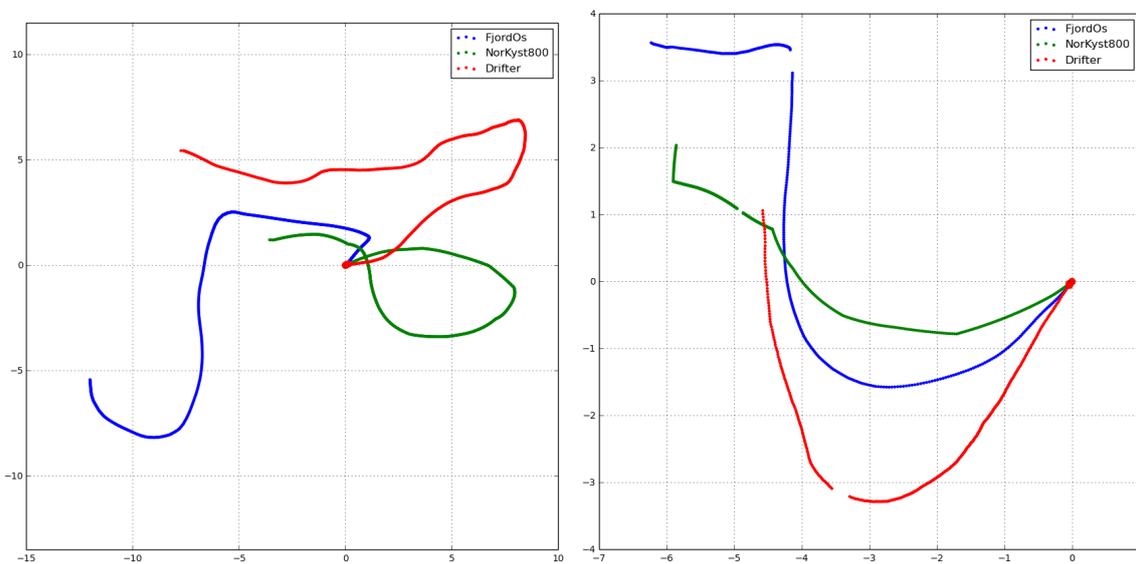

Figure 38: As Figure 35, but displaying drop 101 (left-hand panel, 5 km grid) and drop 102 (right-hand panel, 1 km grid).
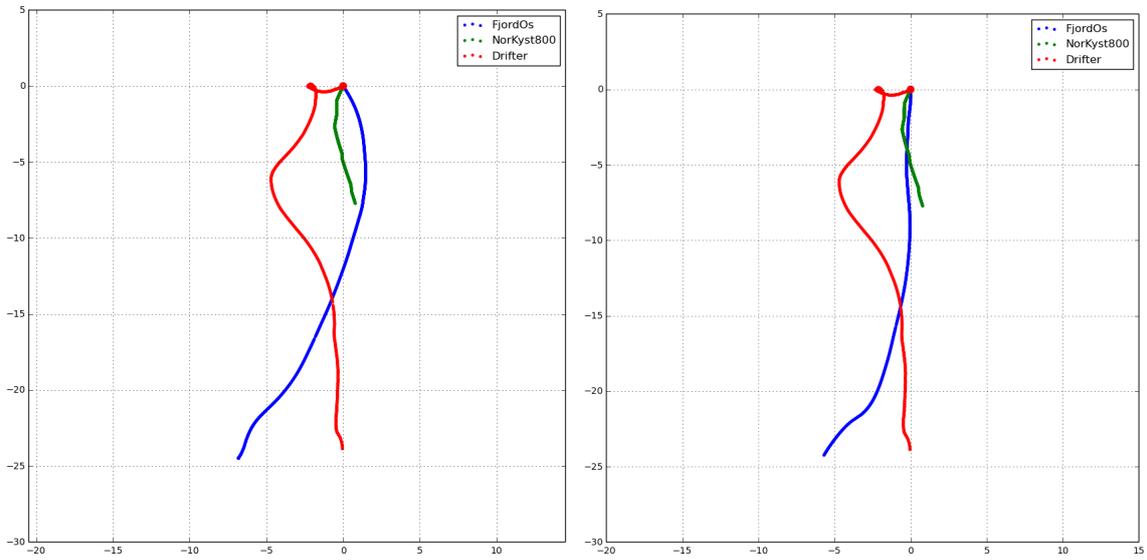
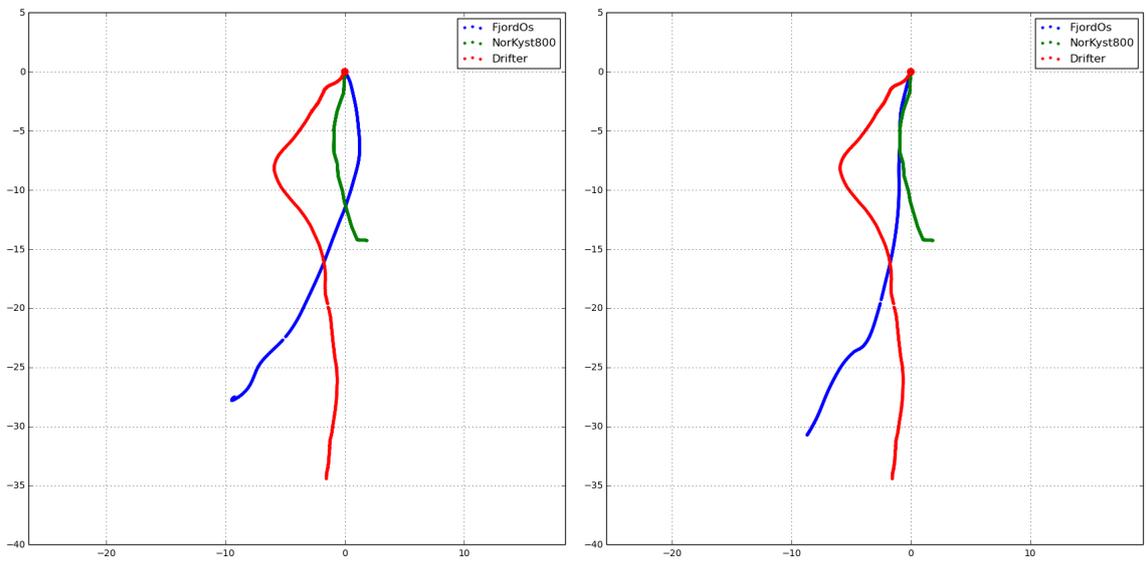Figure 39: As Figure 35, but showing drop 1 of the September 2014 release.

Figure 40: As Figure 39, but for drop 2 2014.

5 Summary and final remarks

Considered is the performance of the FjordOs model, a new circulation model covering the Oslofjord, Norway. The FjordOs model is a version of the Regional Ocean Modeling System (ROMS) as documented by *Haidvogel et al.* (2008) and *Shchepetkin and McWilliams* (2003, 2005, 2009). It is adapted for Oslofjord by utilizing its curvilinear option as detailed in *Røed et al.* (2016). The model is developed to improve the ocean input (e.g., currents) to emergency models used to predict pathways of oil and/or other effluents. The utilization of the curvilinear option in ROMS was chosen to increase the resolution without inflating the computer demand.

The model has earlier been assessed to evaluate its representation of the tidal elevations (*Hjelmervik et al.*, 2017). They found that the tidal elevation is well represented in the model. This finding is underscored by the present study, in which we focus on an evaluation of the model's rendition of the circulation. To this end we compare model results from a near two-year long simulation to observations. The observations encompass water level, currents and temperature at various time periods at fixed stations, and not least observed trajectories of drifters.

In essence currents in the Oslofjord are composed of tidal currents, wind forced currents, currents induced by storm surge events, and currents due to differences in density. The last component is commonly caused by differences in temperature and salinity. It is emphasized that the tides are more often than not the most dominant current in the fjord. The evaluation reveals that the model is not perfect. While the tidal currents are well represented, the currents due to difference in density appears to be less well represented. We find that this lack of success is probably associated with the model's failure in representing a realistic stratification (or baroclinicity). One possibility for the latter weakness may be associate with the use of the coarser mesh model NorKyst800 to initialize the model and the fact that the FjordOs model is forced by the NorKyst800 at its southern open boundary bordering on the Skagerrak throughout the simulation. Thus any lack of success in representing the stratification in the NorKyst800 model will also be reflected in the FjordOs model. Another possibility is the vertical mixing in the model. For instance it appears that the vertical mixing inside of the sill in the Drammensfjord is too vigorous, while the vertical mixing in the outer part of the fjord is too weak.

Nevertheless we argue that its performance is adequate for its purpose. An important justification is that the higher resolution offers a decrease in the number of stranded trajectories compared to models of coarser resolution. Also of importance is that the model provides a realistic representation of the tidal currents and to certain degree the current depth profiles.

Acknowledgements

Appendix

Driftling lanes from the Slagen refinery

A part of the FjordOs project has been to examine how known, and potential, oil spills would spread out in the Oslofjord. The Slagen refinery at Slagentangen is owned by ExxonMobil, and is described as following on their webpage[3]: "Slagen Refinery is situated on the west bank of the Oslofjord about 5 nautical miles south of Horten. The marine terminal consists of a pier about 500 m long with loading/discharging berths on both sides. To the south of the long pier there is a small harbour where mooring boats and oil recovery equipment are kept. The terminal and its near surroundings are owned and controlled by Esso Norge AS. It has its own Harbour Office with Marine Supervisors on duty 24 hours a day." and "The Slagen Marine Terminal has approximately 800 tanker calls a year with size variation 100 to 250 000 DWT. The annual import of Crude oil (mainly from the North sea) and Blendstock is about 6.5 mill. m^3 and about 5.7 mill. m^3 petroleum products are shipped out."

To model the spread of oil from a potential spill at Slagentangen we have used the same approach as in Section 4.5. It is very important to point out that the work done in this appendix is not sufficient to be used for any contingency planning or other work on possible oil spill scenarios. It should be viewed as a "teaser" on possible future work that could be used for contingency planning of unwanted releases of substances from anywhere within the Oslofjord.

Figure 41 shows the release position of the particles used in the simulation marked with a black dot. The left panel show the shortest number of hours from the time of the particle release to a particle is in a given position. The right panel show the corresponding concentrations. When viewing the zoomed in figures (lower figures), it is evident that the coastline of the ocean model does not perfectly match the real coastline, and also the OpenDrift model will at times advect particles onto land. This is linked to the length of the time step used in OpenDrift. A more thorough work on potential oil spills should address these issues. When looking at the area closest to the release position, it clearly shows that most particles are transported towards the southeast, and this is also the direction of which the particles are transported fastest. This compares well to the observations of currents outside Slagen in Figure 19. Figure 42 show the end positions of each trajectory, and the corresponding shortest time from release to that position, and concentration.

This sort of maps could be made and categorised by weather pattern or another known factor, and in turn e.g. be used in the unlikely event of a spill in the time between the spill happening, and

---

[3]http://www.exxonmobil.no/en-NO/company/operations/operating-locations/
slagen-refinery?sc_lang=en-NO, (visited 26.01.2017)

the forecast of oil drift is received.

Figure 41: Slagentangen. Number of hours from particle release, to particle in given area (left panels), and the number of particles that has been inside a given 140x140m area (right panels). Based on one year (April 1st 2015 - April 1st 2016) of simulations, with a maximum lifetime of 15 days of the released particles. This amounts to a total number of 8760 released particles. Please note the different scales of each figure.

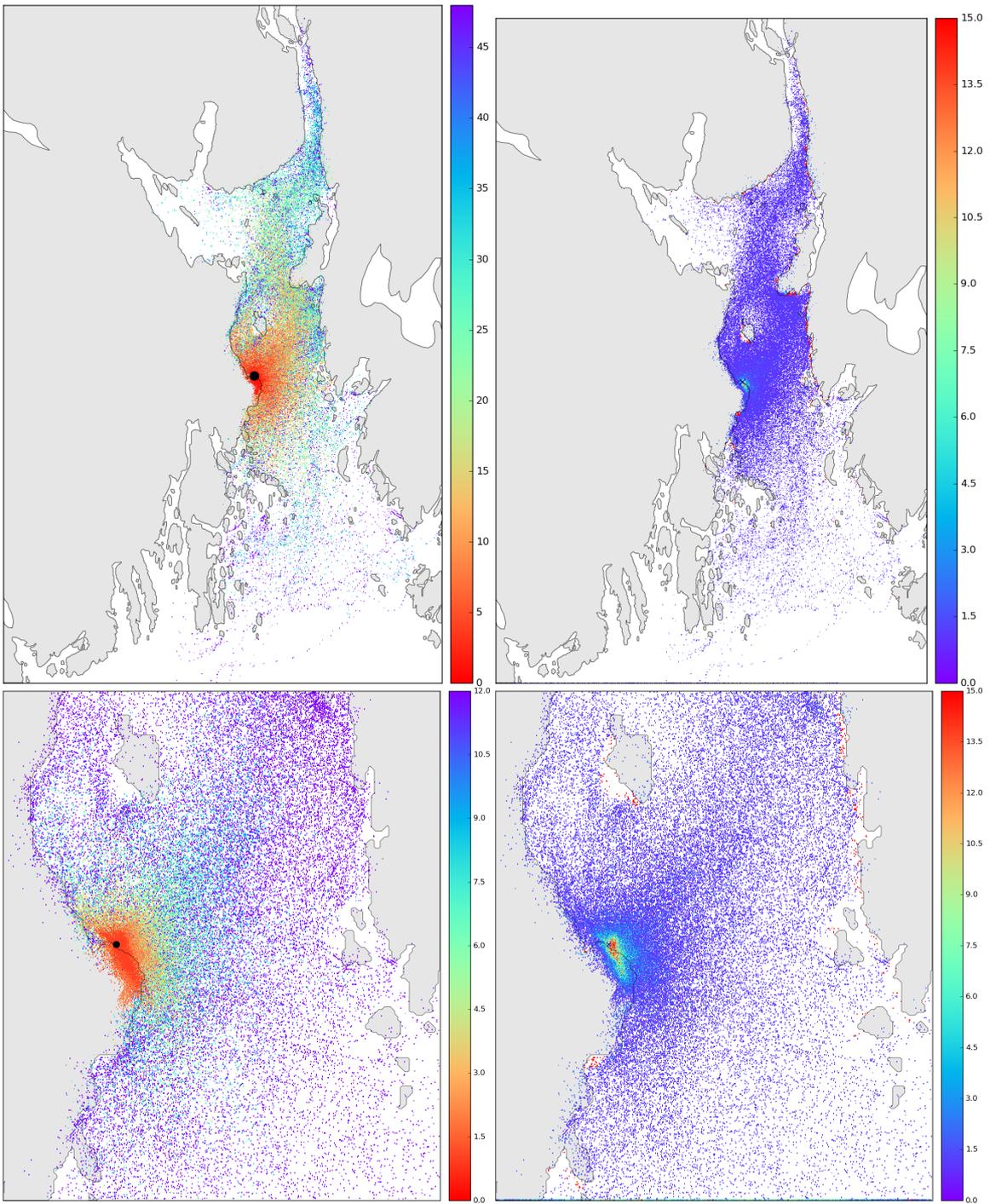Figure 42: Slagentangen. For end position of each trajectory: Number of hours from particle release, to particle in given area (left panel), and the number of particles that has been inside a given 140x140m area (right panel). Based on one year (April 1st 2015 - April 1st 2016) of simulations, with a maximum lifetime of 15 days of the released particles. This amounts to a total number of 8760 released particles. Please note the different scales of each figure.
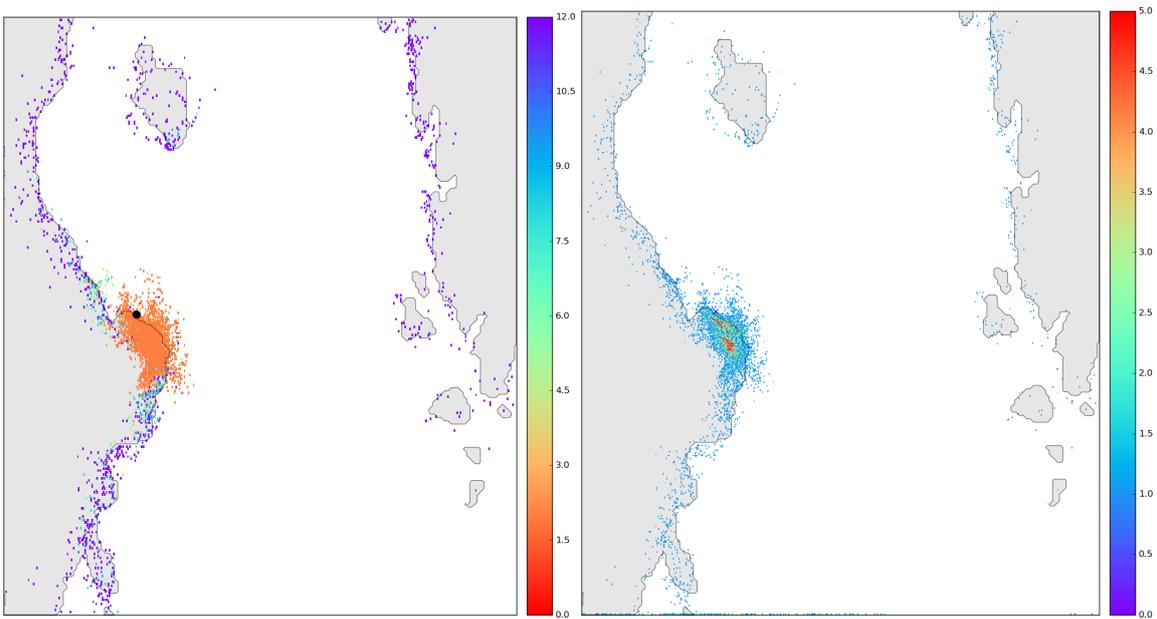
References

Albretsen, J., and L. P. Røed (2010), Decadal long simulations of mesoscale structures in the North Sea/Skagerrak using two ocean models, *Ocean Dynamics*, *60*, 5–36, doi:10.1007/s10236-010-0296-0.

Baalsrud, K., and J. Magnusson (1990), The state of eutrophication in the outer oslofjord 1989 [in norwegian], *Tech. rep.*, Norwegian Institute for Water Research.

Baalsrud, K., and J. Magnusson (2002), *Indre Oslofjord (in Norwegian)*, Fagrådet for Indre Oslofjord.

Berntsen, J., and Ø. Thiem (2007), Estimating the internal pressure gradient errors in a sigma-coordinate ocean model for the Nordic Seas, *Ocean Dynamics*, *57*, 417–429, doi:10.1007/s10236-007-0118-1.

Haidvogel, D. B., H. Arango, P. W. Budgell, B. D. Cornuelle, E. Curchitser, E. D. Lorenzo, K. Fennel, W. R. Geyer, A. J. Hermann, L. Lanerolle, J. Levin, J. C. McWilliams, A. J. Miller, A. M. Moore, T. M. Powell, A. F. Shchepetkin, C. R. Sherwood, R. P. Signell, J. C. Warner, and J. Wilkin (2008), Ocean forecasting in terrain-following coordinates: Formulation and skill assessment of the Regional Ocean Modeling System, *J. Comput. Phys.*, *227*(7), 3595–3624, doi:http://dx.doi.org/10.1016/j.jcp.2007.06.016.

Haney, R. L. (1991), On the pressure gradient force over steep topography in sigma coordinate ocean models, *J. Phys. Oceanogr.*, *21*, 610–619.

Hjelmervik, K., N. M. Kristensen, A. Staalstrøm, and L. P. Røed (2017), A simple approach to adjust tidal forcing in fjord models, *Ocean Dynamics*, pp. 1–10.

Hjelmervik, K. B., N. M. Kristensen, and A. Staalstrøm (2016), Comparison of simulations and observations in the Oslofjord. FjordOs technical report no. 3, *MET Report 13*, Norwegian Meteorological Institute, MET Norway, P.O.Box 43 Blindern, NO-0313 Oslo, Norway.

Klinck, J. M., J. J. O'Brien, and H. Svendsen (1981), A simple model of fjord and coastal circulation interaction, *Journal of Physical Oceanography*, *11*(12), 1612–1626.

Liu, Y., and R. H. Weisberg (2011), Evaluation of trajectory modeling in different dynamic regions using normalized cumulative lagrangian separation, *Journal of Geophysical Research: Oceans*, *116*(C9).

Müller, M., M. Homleid, K.-I. Ivarsson, M. A. Køltzow, M. Lindskog, U. Andrae, T. Aspelien, D. Bjørge, P. Dahlgren, J. Kristiansen, R. Randriamampianina, M. Ridal, and O. Vignes (2017), AROME-MetCoOp: A Nordic convective-scale operational weather prediction model, *Weather and Forecasting*, *32*, 609–627, doi:DOI:http://dx.doi.org/10.1175/WAF-D-16-0099.1.

Pawlowicz, R., B. Beardsley, and S. Lentz (2002), Classical tidal harmonic analysis including error estimates in MATLAB using T_TIDE, *Computers and Geosciences*, *28*(8), 929–937.

Rodhe, J. (1996), On the dynamics of the large-scale circulation of the Skagerrak, *Journal of Sea Research*, *35*(1), 9–21.

Røed, L. P., and I. Fossum (2004), Mean and eddy motion in the Skagerrak/northern North Sea: insight from a numerical model, *Ocean Dynamics*, *54*, 197–220.

Røed, L. P., N. M. Kristensen, K. B. Hjelmervik, and A. Staalstrøm (2016), A high-resolution, curvilinear ROMS model for the Oslofjord. FjordOs technical report no. 2, *MET Report 4*, Norwegian Meteorological Institute, MET Norway, P.O.Box 43 Blindern, NO-0313 Oslo, Norway.

Shchepetkin, A. F., and J. C. McWilliams (2003), A method for computing horizontal pressure-gradient force in an oceanic model with a nonaligned vertical coordinate, *J. Geophys. Res.*, *108*, 3090, doi:10.1029/2001JC001047.

Shchepetkin, A. F., and J. C. McWilliams (2005), The Regional Ocean Modeling System (ROMS): A split-explicit, free-surface, topography-following coordinate ocean model, *Ocean Modelling*, *9*, 347–404.

Shchepetkin, A. F., and J. C. McWilliams (2009), Correction and commentary for "Ocean forecasting in terrain-following coordinates: Formulation and skill assessment of the regional ocean modeling system" by Haidvogel et al., J. Comp. Phys. 227, pp. 3595-3624, *J. Comp. Phys.*, *228*(24), 8985 – 9000, doi:10.1016/j.jcp.2009.09.002.

Staalstrøm, A., and P. Ghaffari (2015), Current conditions in the oslofjord - focus on current strength along the bottom, *Technical Report SNO 6799-2015*, Norwegian Institute for Water Research, NIVA, Gaustadalléen 21, NO-0349 Oslo, Norway.

Staalstrøm, A., and K. Hjelmervik (2017), Strømforholdene i innløpet til Drammensfjorden (in Norwegian), *Vann*, *1*(52), 104–115.

Staalstrøm, A., and L. P. Røed (2016), Vertical mixing and internal wave energy fluxes in a sill fjord, *Journal of Marine Systems*, *159*, 15–32, doi:10.1016/j.marsys.2016.02.005.

Staalstrøm, A., E. Aas, and B. Liljebladh (2012), Propagation and dissipation of internal tides in the Oslofjord, *Ocean Science*, *8*, 525–543.

Svendsen, E., J. Berntsen, M. Skogen, B. Ådlandsvik, and E. Martinsen (1996), Model simulation of the Skagerrak circulation and hydrography during SKAGEX, *Journal of Marine Systems*, *8*(3), 219–236.